The Role of Nuclear Factor kappaB Subunit p50 in Melanoma Pathogenesis

by

KAI GAO

A THESIS SUBMITTED IN PARTIAL FULFILLMENT OF
THE REQUIREMENTS FOR THE DEGREE OF

MASTER OF SCIENCE

in

THE FACULTY OF GRADUATE STUDIES
(Experimental Medicine)

THE UNIVERSITY OF BRITISH COLUMBIA

August 2007

© KAI GAO, 2007

Abstract

Transcriptional factor NF-κB family has been demonstrated to play an important role in tumor pathogenesis and serve as a potential target in cancer therapy. However, it is necessary to clarify the specific functions of NF-κB members, which would provide the basis for the selective blockade and reduction of therapeutic side effects resulting from unspecific inhibition of NF-κB members.

We firstly explored the role of NF-κB p105/p50 in melanoma pathogenesis *in vivo*. We found that the expression of NF-κB p105/p50 significantly increased in dysplastic nevi, primary melanoma and metastatic melanoma compared to normal nevi (p=0.0004, χ^2 test). NF-κB p105/p50 nuclear staining increased with melanoma progression and strong NF-κB p105/p50 nuclear staining was inversely correlated with disease-specific 5-year survival of patients with tumor thickness >2.0 mm (p=0.014, log-rank test). Multivariate Cox regression analysis revealed that nuclear expression of NF-κB p105/p50 is an independent prognostic factor in this subgroup. Moreover, we found that upregulation of NF-κB p50 enhanced melanoma cell migration whereas siRNA knockdown inhibited cell migration. In addition, overexpression of NF-κB p50 induced RhoA activity and Rock-mediated formation of stress fiber in melanoma cells.

To further elucidate how NF-κB p50 is involved in melanoma, we analyzed the gene expression profile in melanoma cells overexpressing NF-κB p50 by cDNA microarray. We found that *IL-6* mRNA was highly induced by NF-κB p50. Since IL-6 is a newly reported proangiogenic factor in cancer, we hypothesized that NF-κB p50 could promote melanoma angiogenesis by

upregulating IL-6. Indeed, using the proliferation assay of human umbilical vein endothelial cells (HUVECs) we demonstrated that the conditioned medium from melanoma cells overexpressing NF-κB p50 promoted HUVEC proliferation *in vitro. In vivo* matrigel plug assay showed that tumor vascularity was significantly enhanced by NF-κB p50. Furthermore, silence of NF-κB p105/p50 decreased IL-6 expression and overexpression of ATF3 abrogated the effect of NF-κB p50 on the induction of IL-6.

Taken together, our data indicate that NF-κB p105/p50 may be an important marker for human melanoma progression and prognosis as well as a potentially selective therapeutic target.

Table of contents

List of tables

List of figures

List of symbols and abbreviations

ATF3	Activating transcription factor 3
CDK2	Cyclin-dependent kinase 2
CMV	Cytomegalovirus
ECGS	Endothelial cell growth supplement
ELISA	Enzyme-linked immunosorbent assay
GAPDH	Glyceraldehyde-3-phosphate dehydrogenase
GST	Glutathione S-transferase
HUVEC	Human umbilical vein endothelical cells
ICAM-1	Intercellular adhesion molecular-1
IL-1 A	Interleukin 1 alpha
IL-6	Interleukin 6
IL-8	Interleukin 8
MAPK	Mitogen-activating protein kinase
MMPs	Matrix metalloproteinases
MYBPC1	Myosin-binding protein C, slow-type
NF-κB	Nuclear factor kappaB
NGAL	Neutrophil gelatinase-associated lipocalin
NLS	Nuclear localization sequence
PAGE	Polyacrylamide gel electrophoresis
PBS	Phosphate buffered saline
PVDF	Polyvinylidene difluoride
RNA	Ribonucleic acid
RNAi	RNA interference
RT-PCR	Reverse transcriptase-polymerase chain reaction
S100B	S-100 protein, beta chain
RHR	Rel homology region
shRNA	Short hairpin RNA
SLC14A1	Urea transporter
SRB	Sulforhodamine B
SULF1	Extracellular sulfatase Sulf-1
TBS	Tris buffered saline
TCA	Trichloroacetate
TMA	Tissue microarray
TRIM9	Tripartite motif protein 9
VCAM-1	Vascular cell adhesion molecular-1
VEGF	Vascular endothelial growth factor
VIP-R-1	Vasoactive intestinal polypeptide receptor 1

Acknowledgements

I would like to express my gratitude to the UBC Faculty of Graduate Study, Department of Medicine, Department of Dermatology and Skin Science and BC Foundation for Non-Animal Research – Evelyn Martin for their support.

I am deeply indebted to my supervisor, Dr. Gang Li, whose scientific thinking, stimulating suggestions and encouragement helped me in all the time of research and writing of this thesis. I am also obliged to my supervisory committee members Dr. Michael Cox and Dr. Bill Salh, as well as Dr. Kevin McElwee, Dr. Andrew Weng, Dr. Vincent Duronio for their guidance, and Dr. Magda Martinka for help in evaluation of TMA staining.

Finally I wish to express my warm thanks to the past and present members of Dr. Li's laboratory (Eric Campos, William Kuo, Marco Garate, Yemin Wang, Ronald Wong, Jun Li, Derek Dai, Philip Ng, Fuqu Lu and Alison Karst) for their valuable support.

To each of the above, I extend my deepest appreciation.

Dedication

This thesis is dedicated to my parents whose love and nurturing made this all possible.

Also, this thesis is dedicated to my wife, Yanshuang Xie, who has been a great source of emotional motivation and inspiration.

Chapter 1. General Introduction

1.1 Cutaneous Melanoma

The human skin consists of three major layers: epidermis, dermis and the subcutaneous layer. The epidermis is the thin outer layer of the skin, which can be divided into three sub-lays. The horny layer, the majority of which is consisted of dead keratinocytes, protects the body from external stresses. Below is a layer of living suprabasal keratinocytes. The basal layer is the inner layer of the epidermis, which contains melanocytes. The dermis consists of blood and vessels, hair follicles, sweat glands and touch & pain receptors. The subcutaneous layer functions as conservation of body heat and shock absorber.

Cutaneous melanoma arises from melanocytes in skin. Classically, the development of melanoma was depicted in five distinct steps. The first step is common nevus followed by dysplastic nevus that shows an increased level of structural and architectural atypia. Then the malignant stage of melanoma appeared as the third step, which was also defined as radial growth phase (Gray-Schopfer, Wellbrock et al. 2007) primary melanoma. The cells in this stage are locally invasive, but deficient of metastatic capacity. Radial growth phase cells can evolved into vertical growth phase (VGP) primary melanoma lesions, which is the fourth step in progression, so that melanoma cells invade into deeper dermis and underlying subcutaneous tissue and the rapid metastasis to almost any organ. According to this model, melanocytic lesions may be divided into benign nevi (i.e., junctional nevi, compound nevi), lesions with possible malignant potential (i.e., dysplastic nevi), and malignant lesions

(i.e., primary melanoma and metastatic melanoma) (Gray-Schopfer, Wellbrock et al. 2007).

Cutaneous malignant melanoma is the most fatal form of skin cancer, and its incidence has increased by 3-8% annually in the Caucasian population (Becker, Kirkwood et al. 2006). In 2006, there were 62,190 estimated new cases of melanoma and ~7,910 patients died from this disease in the United States (Jemal, Siegel et al. 2006). Although the survival rate of newly diagnosed melanoma cases has greatly improved, patients with metastatic melanoma have a very poor prognosis with average survival of 6 to 10 months (Jemal, Thomas et al. 2002; Eigentler, Caroli et al. 2003).

1.2 The role of NF-κB in melanoma

1.2.1 NF-κB family members

It is well-known that the NF-κB family is comprised of five mammalian members: Rel A/p65, RelB, NF-κB1 p105/p50 and NF-κB2 p100/p52. Active form of NF-κB subunit p50 and p52 are produced by ubiquitin-dependent proteolytic process of the c-terminal domain of NF-κB1 p105 and NF-κB2 p100, respectively. All the NF-κB family members share a highly conserved 300-amino acid Rel homology region (RHR). The RHR is important for dimerization, DNA binding and interaction with IκB proteins. A nuclear localization sequence (NLS) also exits within RHR. The classic p65/p50 heterodimer is the predominant form of NF-κB in most cell type. Different dimers formed by NF-κB subunits exhibit different binding affinities for κB

binding site, GGGRNNYYCC (R is pyrimidine and N is any base) (Karin and Ben-Neriah 2000).

The homo- or heterodimers of NF-κB were sequestered by IκBs in cytoplasm. The activation of NF-κB dimers in response to stimuli results in phosphorylation and degradation of IκBs, thus allowing NF-κB to translocate to the nucleus, where it regulates a wide variety of gene expression (Ghosh, May et al. 1998; Natoli, Saccani et al. 2005).

1.2.2 NF-κB in melanoma development

The first evidence of NF-κB in cell transformation comes from the observation that the avian reticuloendotheliosis virus stain-T oncogene product, v-Rel, is derived from the NF-κB protein, c-Rel. In mammalian cells, NF-κB activity is required for Ha-Ras-induced cellular transformation (Finco, Westwick et al. 1997). In addition, oncogenes such as c-myc and Pim-2 are regulated by NF-κB activities (Kim, Gazourian et al. 2000; Fox, Hammerman et al. 2003).

Since NF-κB is related to cellular transformation and many oncogenes, NF-κB is found to be constitutively active in many cancer types including leukemia, breast cancer, and prostate cancer (Sovak, Bellas et al. 1997; Feinman, Koury et al. 1999; Suh and Rabson 2004). In melanoma, elevated NF-κB activity was found in melanoma cell lines (McNulty, Tohidian et al. 2001; Yang and Richmond 2001). NF-κB subunit RelA and phosphorylated RelA were overexpressed while its inhibitor IkappaB-alpha expression is significantly low in melanoma biopsies (McNulty, del Rosario et al. 2004). Interestingly, p16INK4A and NF-κB p65 expression were inversely correlated from nevi to primary and metastastic melanoma, suggesting that NF-κB could

inactivate tumor suppressor p16INK4A in the early stage of melanoma development (Ghiorzo, Mantelli et al. 2004).

1.2.3 NF-κB in melanoma cell proliferation

It is well-known that cyclins and Cdks tightly control cell cycle. NF-κB has been shown to upregulate cyclin D1 expression facilitating cell transition from the G1 phase to S phase. In addition, numerous cytokines or their receptors regulated by NF-κB are growth factor for tumor cells while these cytokines exert their biology functions through NF-κB activity. For example, epidermal growth factor (EGF) receptor was upregulated by NF-κB (Ling, Wang et al. 2004). Activation of epidermal growth factor (EGF) receptor by the binding to EGF leads to NF-κB nuclear translocation and an increase in NF-κB-dependent gene transcription (Haussler, von Wichert et al. 2005). The inhibition of epidermal growth factor causes a reduction of NF-κB activity in melanoma cells (Ivanov and Hei 2005). Furthermore, NF-κB serves as a downstream of many signal pathways such as MAP kinase pathway, transferring proliferation signals from plasma membrane to the nuclei and resulting in cell growth (Ueda and Richmond 2006).

1.2.4 NF-κB in melanoma apoptosis and chemoresistance

Melanoma is notoriously refractory to all standard anticancer therapies. The only FDA-approved drug for the treatment of malignant melanoma, dacarbazine (DTIC), only have remission rate of 5-10% on melanoma patients (Serrone, Zeuli et al. 2000). Although clinic trials have tested a number of anticancer strategies including surgery, immunotherapy, radiotherapy and

chemotherapy, the total response rates are disappointing (Grossman and Altieri 2001; Ballo and Ang 2003; Hersey 2003).

Numerous studies focus on the altered apoptotic pathways in melanoma, looking for the potential targets for novel therapies (Soengas and Lowe 2003). Among the signal pathway impacting melanoma survival, NF-κB pathway has received considerable attention since it was considered "at the crossroads of life and death (Karin and Lin 2002). NF-κB has shown to modulate the expression of factors that were involved in mitochondrial and extrinsic pathways. NF-κB upregulates expression of c-IAP1, c-IAP2, TRAF1/2 as well as Bcl-X_L (Baldwin 1996; Deveraux, Roy et al. 1998; Ravi, Bedi et al. 2001). TRAIL-induced apoptosis is suppressed by NF-κB in melanoma cells (Franco, Zhang et al. 2001). Targeting NF-κB by increasing IκB activity rendered the melanoma cell susceptible to TNF-induced apoptosis (Bakker, Reed et al. 1999). In addition, NF-κB was involved in the MDR1 gene expression, contributing to the chemoresistance of cancer cells (Kuo, Liu et al. 2002).

1.2.5 NF-κB in melanoma cell migration, invasion and metastasis

The fatality of cancer patients is mainly caused by the formation of metastasis rather than by the primary tumor itself. The process of metastasis is highly complicated, which consists of multiple but interrelated steps. Theoretically, the first step is local invasion, which requires tumor cell detach from the primary tumor, become motile and invade into surrounding tissues. Intravasation is the second step. Tumor cells penetrate the blood or lymphatic vessels and finally colonize the metastatic site (Ara and DeClerck 2006).

Therefore, tumor cell migration, invasion and adaptation of new environment are three interrelated events corresponding to distinct gene expressions in tumor cells and interaction between tumor cells and different stromal cells (Labrousse, Ntayi et al. 2004).

Previous studies have demonstrated that NF-κB was highly involved in dynamics of melanoma metastasis. The constitutive activity of NF-κB plays a major role in the endogenous expression of chemokines such as CXCL1 and CXCL8. These chmokines further activate NF-κB in tumor cells. When CXCL1 antibody was applied to neutralize CXCL1, NF-κB activity was reduced by ~50%. In addition, CXCL8 expression correlated with the aggressiveness of melanoma. Overexpression of CXCL8 in melanoma cells increases their metastatic potential (Kunz, Hartmann et al. 1999; Yang and Richmond 2001). On the other hand, both PI3K pathway and GTPase (RhoA, cdc42 and Rac1) phosphorylate IκB and translocate p65/p50 or p50/p50 dimers to the nucleus, promoting stress fiber formation and cell migration (Perona, Montaner et al. 1997; Montaner, Perona et al. 1998; Jimenez, Portela et al. 2000).

Invasion of tumor cells requires the degradation of matrix and penetration of stroma (Labrousse, Ntayi et al. 2004), which also required NF-κB activity. NF-κB regulates the expression of matrix metalloproteinases (MMPs), urokinase type of plasminogen activator (uPA) and IL-8, all of which are critical factors in tumor invasion and metastasis (Novak, Cocks et al. 1991; Bond, Fabunmi et al. 1998; Borghaei, Rawlings et al. 2004; Jenkins, Mikhail et al. 2007). MMP-9 was mainly expressed in thin malignant melanoma lesions (thickness less than 1.6mm), suggesting its role in the initiation stage of melanoma development (van den Oord, Paemen et al. 1997). Inhibition of NF-

κB activity reduces MMP-9 transcription (Bond, Fabunmi et al. 1998). uPA is another important protease involved in tumor invasion, which seems to be specifically regulated by NF-κB subunit RelA (Wang, Abbruzzese et al. 1999).

In addition, NF-κB modulates the expression of a few adhesion molecules involved in mestastasis, including ICAM-1, VCAM-1 and ELAM-1 (E-selectin) (Whelan, Ghersa et al. 1991; Iademarco, McQuillan et al. 1992; van de Stolpe, Caldenhoven et al. 1994). The inducible nitric oxide synthase (iNOS) and Cox-2 have been closely linked to metastatic potential of tumor, which are also regulated by NF-κB (Thomsen and Miles 1998; Denkert, Kobel et al. 2001).

1.2.6 NF-κB in melanoma angiogenesis

Angiogenesis is a process involving the growth of new blood vessels, which is essential for tumor growth, invasion and metastasis (Hanahan and Weinberg 2000). Melanoma is well-known for its active formation of new blood vessels even back to the earliest days of tumor angiogenesis research (Warren and Shubik 1966). A prospective study of 417 cutaneous melanomas revealed that the most important determinant of overall survival is tumor vascularity, suggesting the important role of angiogenesis in melanoma progression (Kashani-Sabet, Sagebiel et al. 2002). Another matched-pair melanoma tissue array analysis revealed a significant correlation between overexpression of NF-κB p65 and development of tumor vascularity, indicating the important role of NF-κB in angiogenesis (Kashani-Sabet, Shaikh et al. 2004).

The major pro-angigenic factor regulated by NF-κB is vascular endothelial growth factor (VEGF) (Levine, Lucci et al. 2003). VEGF

expression was found to be associated with the transition of horizontal to vertical growth phase in melanoma (Erhard, Rietveld et al. 1997). In addition, NF-κB targets genes including IL-8, which promotes melanoma angiogenesis. *ING4* tumor suppressor gene directly interacts with NF-κB subunit RelA and inhibits the expression of IL-8 and cyclooxygenase 2 (COX2) (Garkavtsev, Kozin et al. 2004). Inhibition of IL-8 produced by cancer cells prevents tumor angiogenesis (Sparmann and Bar-Sagi 2004).

1.3 The role of IL-6 in melanoma

1.3.1 The signal pathway of IL-6

Interleukin-6 (IL-6) is a pleiotropic factor and functions extensively in immune and hematopoietic system as well as cardiovascular and nervous systems. Classically, IL-6 binds to its receptor (IL-6R), triggering homo- or hertero-dimerization of gp130. Then the dimmerization causes phosphorylation of gp130 and transcription factors STAT1/STAT3 by Janus-Kinases (JAK1, JAK2, TYK2). Activation of STAT3 leads to upregulation of inhibitory proteins of the suppressor of cytokine signaling (SOCS) family. Furthermore, dimerization of gp130 links to MAP-kinase pathway, resulting in activation of transcription factor NF-IL-6 and AP-1 (Taga and Kishimoto 1997; Heinrich, Behrmann et al. 2003).

Alternatively, the complex of soluble IL-6 receptor (sIL-6) and IL-6 is capable of mediating signal transduction on cells that do not express membrane-bound IL-6R, which is called trans-signalling. Therefore, the complex sIL-6/IL-6R not only enhances the effect of IL-6 due to bypass the

limit of the amount of IL-6R, but also greatly widens the potential of IL-6 to target multiple cell types including tumor cells. Furthermore, biological effect of sIL-6/IL-6R complex could only be limited by soluble gp130 or its analog, but not mutation or absence of gp130 in the cell membrane (Jones, Horiuchi et al. 2001; Kallen 2002).

1.3.2 IL-6 in melanoma proliferation and angiogenesis

In the context of cancer, IL-6 has been demonstrated to be involved in cancer cell apoptosis, proliferation, angiogenesis and metastasis. It is well-known that IL-6 is a growth factor in multiple myeloma (Kawano, Hirano et al. 1988). However, IL-6 plays a dual role in melanoma cell proliferation. IL-6 induced growth arrest of melanoma cells derived from early-stage (radical growth phase or metastatically incompetent) while those cells from advanced stage (metastatically competent) were stimulated by IL-6. Studies also show that IL-6 induces p21 expression in sensitive melanoma cells instead of resistant cells (Cornil, Theodorescu et al. 1991; Lu and Kerbel 1993; Florenes, Lu et al. 1999).

Although there is no direct evidence linking IL-6 to melanoma angiogenesis at this time, studies on other cancer types clearly show that IL-6 is a pro-angiogenic factor. Ovarian cancer cells secrete IL-6 when they were implanted into the peritoneal cavity of female nude mice. Additionally, IL-6 dramatically enhances endothelial cell migration *in vitro* and vascularization *in vivo* (Nilsson, Langley et al. 2005; Yao, Zhai et al. 2006). Inhibition of IL-6 signalling by direct targeting IL-6 or its receptor significant suppresses tumor angiogenesis through decreasing tube formation and blood vessel formation

of endothelial cells in gastric carcinoma and cervical carcinoma (Huang, Wu et al. 2004; Su, Lai et al. 2005). Thus the role of IL-6 in angiogenesis seems mainly dependent on activation of endothelial cells by IL-6.

1.4 Hypothesis and thesis theme

Since constitutive activity of NF-κB was involved in development and malignancy of many cancer types and NF-κB subunit p50 is a predominant component of NF-κB dimmer, we hypothesize that NF-κB subunit p50 plays an important role in melanoma pathogenesis.

The main objectives in the thesis are to : 1) investigate the *in vivo* role of NF-κB p50 in human melanoma; 2) investigate the *in vitro* role of NF-κB p50 in melanoma cells; 3)to determine the downstream of NF-κB subunit p50 and its function in melanoma. The first objective was met by observing the prognostic significance of p50 in melanoma using tissue microarray technology and statistic analysis. The second objective was met by demonstrating that p50 promotes melanoma cell migration and stress fiber formation via RhoA-Rock pathway. The third objective was met by identifying that *IL-6* is the main downstream of p50 using cDNA microarray and p50 enhances angiogenesis in melanoma through upregulation of IL-6 expression.

Chapter 2. Materials and methods

2.1 Tissue microarray construction

The construction and composition of the melanoma TMA were described previously (Dai, Martinka et al. 2005). Briefly, formalin-fixed, paraffin-embedded tissue blocks containing 16 normal nevi, 66 dysplastic nevi, 204 primary melanomas and 58 metastatic melanomas were retrieved from the 1990–1998 archives of the Department of Pathology, Vancouver General Hospital. The use of human skin tissues in this study was approved by the medical ethics committee of the University of British Columbia and was performed in accordance with the Declaration of Helsinki Guidelines. For each case, the most representative tumor area was selected and marked on hematoxylin and eosin stained slides. The TMAs were assembled using a tissue-array instrument (Beecher Instruments, Silver Spring, MD). Duplicate 0.6-mm-thick tissue cores were taken from each biopsy specimen. Three composite high-density TMA blocks containing 107, 126, and 111 cases from a total of 344 patients were designed. Multiple 4-μm sections were cut with a Leica microtome (Leica Microsystems Inc, Bannockburn, IL) and transferred to adhesive-coated slides. One section from each TMA was routinely stained with hematoxylin and eosin. The remaining sections were stored at room temperature for immunohistochemical staining.

2.2 Immunohistochemistry

TMA slides were deparaffinized by heating at 55°C for 30 min followed by three washes with xylene. Tissues were rehydrated in a series of ethanol

washes and rinsed with PBS. Antigen retrieval was carried out by microwaving the slides at high power in 10 mM citrate buffer (pH 6.0) for 4 min. Endogenous peroxidase activity was quenched with 0.3% hydrogen peroxide in PBS for 20 min. Non-specific binding was blocked with normal goat serum for 30 min. NF-κB subunit p105/p50 immunoreactivity was studied using the polyclonal rabbit anti-p50 antibody (Santa Cruz Biotechnology, Santa Cruz, CA) at a dilution of 1:500. The antibody was applied for 1 h at room temperature. The slides were washed with PBS for three times and then incubated with a biotinylated anti-rabbit antibody (Santa Cruz Biotechnology) for 30 min. After washing with PBS, the slides were incubated with horseradish peroxidase-conjugated streptavidin (Santa Cruz Biotechnology) for 45 min. Following the wash with PBS, the signals were developed with 3,30-diaminobenzidine substrate (Vector Laboratories, Burlington, ON, Canada) for 5 min and counterstained with hematoxylin. The slides were dehydrated and sealed with coverslips. Negative control was performed by omitting the primary p105/p50 antibody.

2.3 Evaluation of immunostaining

Due to loss of biopsy cores or insufficient tumor cells present in the cores, 14 cases of normal nevi, 51 cases of dysplastic nevi, 185 cases of primary melanomas, and 55 cases of melanoma metastases could be evaluated for p105/p50 staining. The p105/p50 staining in TMAs was examined blinded by three independent observers (including one dermatopathologist) simultaneously, and a consensus score was reached for each core. The positive reaction of p105/p50 was scored into four grades according to the

intensity of the staining: 0, 1+, 2+, and 3+. The percentages of p50/p105 staining were also scored into four categories: 1 (0-25%), 2 (26-50%), 3 (51-75%), and 4 (76-100%). For cases in which multiple biopsy cores were available, 80% of the biopsies had uniform staining. In the cases with a discrepancy between duplicated cores, the average score from the two tissue cores was taken as the final score. The sum of the intensity and percentage scores is used as the final staining score (Dai, Martinka et al. 2005). The staining pattern of the biopsies was defined as follows: 1, negative; 2 to 3, weak; 4 to 5, moderate; 6 to 7, strong. In addition, the percentage of cells showing positive staining in the nucleus was assessed. We classified the nuclear staining as strongly positive if >50% of cells contained NF-κB p105/p50 in the nuclear compartment, and weakly positive if ≤50% of cells show NF-κB p105/p50 in the nucleus.

2.4 Statistical analysis of TMA

Statistical analysis was performed with the SPSS 11.5 software (SPSS, Chicago, IL). The χ^2 test was used to compare the quantitative differences of p105/p50 staining in various stages of melanoma progression. The Kaplan-Meier method and log-rank test were used to evaluate the correlations between p105/p50 expression and patient survival. Cox regression model was used for multivariate analysis. A p value of less than 0.05 was considered significant.

2.5 Cell culture

MMRU and Sk-mel-3 human melanoma cell lines were cultured in Dulbecco's Modified Eagle Medium supplemented with 10% fetal bovine serum (FBS) (Invitrogen, Burlington, ON, Canada). The human umbilical vein endothelical cells (HUVECs), provided by Dr. A. Karsan (University of British Columbia), were cultured in Ham's F12K medium supplemented with 2 mM L-glutamine, 0.1 mg/ml heparin, 0.03–0.05 mg/ml endothelial cell growth supplement (BD Biosciences, Mississauga, ON Canada), and 10% FBS (Ma, del Soldato et al. 2002). All cells were maintained in 5% CO_2 atmosphere at 37°C

2.6 Transfection and infection

Cells were grown to 70-80% confluency in 6-well plates before plasmids and siRNA transfection. Cells were transient transfected with expression vector pCMV or pCMV-hp50 encoding human NF-κB p50 (Guan, Hou et al. 2005) by lipofectamine reagent (Qiagen, Mississauga, ON, Canada) according to the manufacturer's instructions. Twenty hours after transfection, the medium containing transfection reagents was removed. The cells were rinsed twice with PBS and incubated in fresh medium. For siRNA transfection, cells were incubated with non-specific control siRNA or NF-κB p105 siRNA (Qiagen) in serum-free medium for 20 h, followed by incubation in the complete medium supplemented with 10% FBS (Invitrogen). The cells were harvested at different time points and lysed for Western blot assay.

The transfection and generation of stable clones overexpressing p50 were performed as previously described (Wang and Li 2006). MMRU melanoma cells were transfected with expression vector pCMV or pCMV-hp50

and incubated at 37°C for 48 h followed by a 14-day selection in the culture medium supplemented with 800 μg/ml of G418 (Sigma). Single clones were then picked up and maintained in the culture medium containing 100 μg/ml of G418.

The lentivirus expressing NF-κB p105 shRNA (MISSION shRNA Lentiviral) and shRNA control particle were purchased from Sigma (St. Louis, MO). The target sequence of NF-κB p105 shRNA was 5'-CCGGCGAATGACA GAGGCGTGTATACTCGAGTATACACGCCTCTGTCATTCGTTTTT-3'. The procedure of infection and establishment of shRNA stable clone was performed according to the supplier's recommendation. Briefly, MMRU melanoma cells were seeded in 24-well plates at a density of 3×10^4 cells/well. After 24 h, virus stock was added to the cell cultures at a multiplicity of infection (MOI) of 5. Media were changed 16 h post-infection. Positive stable clones were selected by puromycin at the concentration of 1 μg/ml 48 h after infection. Then the clones were transferred to 6-well plates and maintained in 0.5 μg/ml of puromycin (Sigma).

2.7 Western blot assay and ELISA

Cells were washed with PBS three times, and lysed in triple detergent buffer (50 mM Tris-Cl [pH 8.0], 150 mM NaCl, 0.02% sodium azide, 0.1% SDS, 100 μg/ml phenylmethylsulphonyl fluoride, 1 μg/ml aprotinin, 1% Nonidet P-40, 0.5% sodium deoxycholate) for 20 min on ice. The lysate was centrifuged at 12,000× *g* for 10 min and the supernatant was collected. The protein concentration was determined by the DC Protein Assay (Bio-Rad, Mississauga, Ontario, Canada). 30 μg/lane of proteins were separated on

10% polyacrylamide/SDS gels and electroblotted onto polyvinylidene difluoride filters. The filters were then blocked with 5% skimmed milk for 1 h and incubated with polyclonal rabbit anti-p105/p50 (1:500) (Santa Cruz Biotechnology), polyclonal rabbit anti-p65 antibody (1:500) (Santa Cruz Biotechnology), or monoclonal mouse anti-actin (1:1,000) (Sigma, St. Louis, MO) for 1 h at room temperature, and then incubated with horseradish peroxidase-conjugated secondary antibody for 1 h at room temperature. The signals were detected with enhanced chemiluminescence (Amersham Biosciences, Piscataway, NJ). The band intensity was analyzed by Image J 1.37v software (NIH). IL-6 concentration in conditioned medium was measured by the ELISA kit (eBioscience, San Diego, CA) and performed according to the manufacturer's instructions.

2.8 Wound healing assay

After MMRU and Sk-mel-3 melanoma cells were transfected with plasmids or siRNA, cells were cultured in fresh medium for 24 h and treated with 10 μg/ml mitomycin C (Sigma) for 2 h. After washing with PBS, a standard 200-μl pipette tip was drawn across the center of each well to produce a wound of approximately 0.5-mm in width. The wounded monolayers were washed twice to remove non-adherent cells and fresh medium was added. The photographs were taken at the same position of the wounds at various time intervals. The starting wound edges were defined in each photo by white lines according to the scratch at 0 h time point. The numbers of migrating cells across these white lines in the photos were counted to quantitate the rates of migration (Maffucci, Cooke et al. 2005).

2.9 RhoA pull-down assay

MMRU melanoma cells were seeded into 100-mm plates and cultured to 80% confluency. The cells were transfected with vector pCMV or pCMV-hp50 for 20 h, or without transfection as control. Then all cells were serum-starved for 24 h. Transfected cells were incubated with medium containing 10% FBS for 3 minutes at 37°C. Cells were washed with 10 ml of ice-cold TBS (50 mM Tris/HCl [pH 7.5], 150 mM NaCl) and lysed in 300 µl lysis buffer (50 mM Tris/HCl [pH 7.2], 150 mM NaCl, 10 mM $MgCl_2$, 1% (v/v) Triton X-100, 0.5% (w/v) sodium deoxycholate, 0.1% (w/v) SDS, 10 µg/ml each of aprotinin and leupeptin, and 1 mM phenylmethylsulphonyl fluoride). The cell lysates were cleared by centrifugation at 12,000× *g* for 15 min at 4°C. Cell lysates (0.5 mg of protein) in 500 µl lysis buffer were mixed with 20 µg GST-fusion protein immobilized to Glutathione Sepharose 4B beads and the mixture was rotated for 1 h at 4°C. The samples were then washed with lysis buffer three times. Bound proteins were fractionated in 10% SDS/PAGE and immunblotted with monoclonal mouse anti-RhoA antibody (1:200) (Santa Cruz Biotechology). The total cell lysates were also separated on 10% SDS/PAGE and blotted with anti-RhoA antibody to detect total RhoA expression.

2.10 Immunofluorescence

MMRU cells were transfected with vector pCMV or pCMV-hp50 and subcultured onto coverslips in 6-well plates. After 5 h, the cells were serum-starved overnight. Then cells were collected after stimulation with complete medium containing 10% FBS for a desired period of time. The cells were fixed with 2 ml of fixation solution (2% paraformaldehyde, 0.5% Triton X-100 in PBS)

for 30 min at 4°C. After washing with PBS, the cells were incubated with normal goat serum for 1 h, followed by anti–p50 primary antibody for 1 h (Santa Cruz Biotechology) and Cy2-conjugated goat anti-rabbit secondary antibody (Jackson ImmunoResearch, West Grove, PA) for 1 h. The cells were then stained with phalloidin-rhodamine (1 unit per coverslip; Invitrogen) for 30 min. Finally, the coverslips were incubated with 1:3,000 dilution of stock Hoechst 33258 (20 mM) for 10 min and the cells were visualized under a fluorescent microscope. Photos were taken with a cooled mono 12-bit Retiga-Ex camera.

2.11 RNA isolation and microarray analysis

Vector clone or p50-expressing clone M8 were seed in triplicate 100-mm plates at the same density. When reaching 80% confluency, the cells were lysed in Trizol (Invitrogen, Carlsbad, CA) and total RNA was isolated according to the manufacturer's protocol. The quality and quantity of three RNA samples from vector clone and another three RNA samples from M8 were assessed with an Agilent 2100 Bioanalyzer (Agilent Technologies, CA). Microarray of 21,000 (70-mer) human oligos (Operon Technologies, Huntsville, AL) printed in 3x SSC onto Erie aminosilane (Erie Scientific Company, Portsmouth, NH) were supplied by the Microarray Facility of the Prostate Centre at Vancouver General Hospital (Kojima, Mulholland et al. 2006). Total RNA (10 μg) from each sample was reverse transcribed into cDNA incorporating a specific sequence present on the 5' end of the RT primer. The cDNA was hybridized to the array overnight at 50°C. After stringent washing, the fluorescent 3DNA reagent, which includes a "capture

sequence" complementary to the sequence at the 5' end of the RT primer, was hybridized to the cDNA at 53°C for 3 h. Following further washing, the arrays were immediately scanned on a GenePix 4200AL (Molecular Devices, Sunnyvale, CA). Signal quality and quantity were assessed using Imagene 6.0.1 (BioDiscovery, San Diego, CA). Data from Imagene were analyzed on GeneSpring 7.1 (Agilent Technologies) for profiling significant changes. To compare the expression profile of vector clone and p50-expressing clone M8, *t*-test was performed. Hierarchical clustering was performed using Pearson correlation.

2.12 Quantitative real-time PCR and conventional PCR

For validation of array results, cDNA was obtained using a combination of oligo-dT, dNTP mix (10 nM each) and Superscript II (Invitrogen). PCR primers for each gene (IL-6, VIP-R-1, SLC14A1, IL-1A, Megsin, NGAL, S100B, SULF1, TRIM9 and MYBPC1) were designed using Primer Express 3.0 software (Applied Biosystems, Foster City, CA), with a melting temperature at 58–60°C and a resulting product of 100 bp. . The primers used for PCR analysis were: beta actin forward, 5'-GCTCTTTTCCAGCCTTCCTT-3', reverse, 5'-CGGATGTCAACGTCACACTT-3'; IL-6 forward, 5'-AGTCCAGCCTGAGGGCT CTT-3', reverse 5'-GCCCAGTGGACAGGTTTCTG-3'; VIP-R-1 forward, 5'-TCCAAGTCTCAGTGGCTTCATCT -3', reverse 5'-GGAGGGCAGCTCTTGAT TCC-3'; SLC14A1forward, 5'-CTGTTCACGGCCTATCTTGGA-3', reverse 5'-GGAACAATAGCGTGGCCAAA-3'; IL-1A forward, 5'-CATGAAGGCTGCATG GATCA-3', reverse 5'-TGGTTGCTACTACCACCATGCT-3'; Megsin forward, 5'-GCCAAAGTGGAGCGAGT TGA-3', reverse 5'-CGTTCTTGATTTTGCCAT

GTGT-3'; NGAL forward, 5'-CAGGAGAACTTCATCCGCTTC T-3', reverse 5'-TGTGCACTCAGCCGTCGATA-3'; S100B forward, 5'-GGCGATGGAGACCCTCATC-3', reverse 5'-CGTCTGCAGCAGCTCTTTC A-3'; SULF1 forward, 5'-AATGCTGCCCATCCACATG-3', reverse 5'-CATGTTATACAGCCTCTCCACAGAA-3'; TRIM9 forward, 5'-GATGGCAACG GTGGTCAATT-3', reverse 5'-TGACCCGAGCGTTGTATGTG-3'; MYBPC1 forward, 5'-TGCCAGAGAATCCTGTTTATCAATAA-3', reverse 5'- TTACGAA GAGCTCAGTGGAACATT-3'. PCR of each primer was carried out in triplicate in 25 µL using SYBR Green Master Mix (Applied Biosystems) for 15 min at 95°C for initial denaturing, followed by 40 cycles of 95°C for 30 s and 60°C for 30 s in the ABI 7900HT fast real time PCR System.

Conventional PCR was carried out as previously described (Ng, Campos et al. 2004). IL-6 primers for conventional PCR are forward 5'-GCCCTGAGAAAGG

AGACA-3', and reverse 5'-CTGAGGTGCCCATGCTAC-3'. ATF3 primers are forward, 5'-TAAGCAGTCGTGGTATGG-3', and reverse 5'-TGGAGTTGAGGC AAAGAT-3'. Amplification was performed as follow: initial denaturation at 94°C for 3 min, denaturation at 94°C for 1 min, annealing at 55°C for 1 min, and polymerization at 72°C for 1 min. The reaction was repeated for 35 cycles followed by final polymerization at 72°C for 10 min. Samples were then electrophoresed on a 2% agarose gel containing 0.5 µg/ml of ethidium bromide. The IL-6 specific primers generate a 458 bp product as visualized under ultraviolet light.

2.13 Conditioned medium

Cells (2×10^5) were seeded in 6-well tissue culture plates. After 24 h, cells were washed with PBS, and 1.5 ml of DMEM containing 10% FBS was added into each well. After another 24 h, the medium was collected, centrifuged to remove any cell debris and stored at -80°C.

2.14 Sulforhodamine B cell proliferation assay

HUVECs were plated into 24-well plates at a concentration of 2.5×10^4 cells per well. After 24 h, HUVECs were stimulated with different conditioned medium. 48 h later, the medium was removed and cells were fixed with 500 µl of 10% trichloroacetic acid for 1 h at 4°C. The cells were then washed with tap water, air dried, and stained with 500 µl of 0.4% sulforhodamine B (dissolved in 1% acetic acid) for 30 min at room temperature. The cells were destained with 1% acetic acid and air dried. For quantification, the cells were incubated with 500 µl of 10 mM Tris (pH 10.5) on a shaker for 20 min to dissolve the bound dye followed by colorimetric determination at 550 nm with 100 µl aliquots (Wang and Li 2006). Similarly, vector clone and p50-overexpressing clone M6 and M8 were seeded in 24-well plates in triplicate. Cells were washed and fixed with 10% trichloroacetic acid at different time points and the growth rate was determined with sulforhodamine B staining.

2.15 *In vivo* angiogenesis assay

Vector clone or p50-expressing clone M8 (10^6 cells) mixed with 500 µl matrigel (BD Biosciences) were injected s.c. into 4- to 8-week-old nude mice at sites lateral to the abdominal midline, two injections per mouse (one is

vector clone and the other is p50-overexpressing clone M8). Mice were sacrificed 7 days after matrigel injection. The matrigel plugs were recovered and photographed immediately. Plugs then were dissolved in PBS and incubated at 4°C overnight. Hemoglobin levels were measured by Drabkin's solution (Sigma) according to the manufacturer's instructions (Su, Lai et al. 2005; Narita, Staub et al. 2006).

Chapter 3. Identification of prognostic significance of NF-κB subunit p105/p50 in human melanoma

3.1 Rationale

Cutaneous melanoma is the most aggressive skin cancer with its incidence continuing to increase in the Caucasian population (Becker, Kirkwood et al. 2006). In 2006, there were 62,190 estimated new cases of melanoma in the United States (Jemal, Siegel et al. 2006). Although numerous therapeutic strategies including surgery, immunotherapy, radiotherapy and chemotherapy have been tested in clinic trials, the average survival of patients with metastatic melanoma is still 6 to 10 months (Jemal, Thomas et al. 2002; Eigentler, Caroli et al. 2003).

NF-κB has been demonstrated to play an important role in melanoma proliferation, apoptosis resistance, invasion and metastasis (Amiri and Richmond 2005). Cell cycle related factors such as cyclin D1 and cyclin-dependent kinase 2 (CDK2) as well as anti-apoptotic factors such as melanoma inhibitor of apoptosis (ML-IAP), which are all downstream effectors of NF-κB, are shown to be overexpressed in melanoma (Alonso, Ortiz et al. 2004). NF-κB also regulates the expression intercellular adhesion molecule-1 (ICAM-1), vascular cell adhesion molecule-1 (VCAM-1), and matrix metalloproteinases (MMPs) that facilitate the invasion and metastasis of melanoma (Johnson, Stade et al. 1989; Iademarco, McQuillan et al. 1992; Boyano, Garcia-Vazquez et al. 2000; Langley, Carlisle et al. 2001; Borghaei, Rawlings et al. 2004). Recently, inhibition of NF-κB was shown to be a

potential means to sensitize melanoma cells to anticancer drugs (Amiri, Horton et al. 2004).

Despite close association between NF-κB expression and tumor progression, complete inhibition of NF-κB activity may result in severe side effects because NF-κB regulates the expression of over 150 genes, some of which are involved with normal cellular functions such as immune response and cell proliferation (Karin and Lin 2002; Amiri and Richmond 2005; Natoli, Saccani et al. 2005). Lack of selective blockade of NF-κB activity is due to the poor understanding of specific functions of NF-κB family members in different cell types. The NF-κB family is comprised of five mammalian members: RelA/p65, RelB, c-Rel, NF-κB1 p105/p50 and NF-κB2 p100/p52. Active forms of NF-κB subunit p50 and p52 are produced by ubiquitin-dependent proteolytic process of the c-terminal domains of NF-κB1 p105 and NF-κB2 p100, respectively. In most cells, NF-κB subunit forms homo- or heterodimers and sequestered by IκB in cytoplasm. The activation of NF-κB dimers in response to stimuli results in nuclear translocation of the dimers which then regulate a wide variety of gene expression (Ghosh, May et al. 1998; Natoli, Saccani et al. 2005). Thus far, only a few reports showed specific roles of individual NF-κB members under certain circumstances. For example, overexpression of RelA inhibited TRAIL-induced apoptosis, whereas overexpression of c-Rel enhanced this process (Chen, Kandasamy et al. 2003). Depletion of NF-κB subunit RelA led to hepatic cell death and embryonic lethality of mice (Beg, Sha et al. 1995). In human keratinocytes, overexpression of RelA caused cell growth arrest (Dajee, Lazarov et al. 2003).

The p50-homodimer is also known to be responsible for lipopolysaccharide (LPS) tolerance (Ziegler-Heitbrock 2001).

Since recent reports showed that NF-κB subunit p50 was elevated in classical Hodgkin lymphoma (Mathas, Johrens et al. 2005), nasopharyngeal carcinoma (Thornburg, Pathmanathan et al. 2003) and cervical carcinoma (Prusty, Husain et al. 2005), we hypothesize that NF-κB subunit p105/p50 would also play an vital and specific role in melanoma progression.

3.2 Results

3.2.1 Clinicopathological features of TMA

For 185 cases of primary melanoma that NF-κB p105/p50 staining was available, there were 106 male and 79 female. Of 55 cases of metastatic melanoma that were informative, there were 38 male and 17 female. The mean average age of melanoma patients was 57-y ranging from age 21 to 92. Breslow thickness, which is the distance measured from the top layer of epidermis to the deepest point of tumor penetration, was used as the criteria for melanoma staging (Marghoob, Koenig et al. 2000). Among 185 cases of primary melanoma, 55 were ≤1 mm, 81 were 1.1-2.0 mm, 23 were 2.1-4.0 mm, and 26 were >4.0 mm. Superficial spreading melanoma accounted for 79 cases, lentigo maligna melanoma 25 cases, and the remaining 81 cases consisted of nodular melanoma, acrolentigous melanoma, and desmoplastic melanoma. The majority of the primary melanomas were isolated from sun-protected sites (146 cases; trunk, arm, leg, and feet) and 59 cases were obtained from sun-exposed sites (head and neck). Tumor ulceration was observed in 28 cases (Table 3-1).

3.2.2 NF-κB p105/p50 nuclear expression correlates with melanoma progression

To investigate the expression level of NF-κB p105/p50 in the biopsies of pigmented lesions, immunohistochemical staining of normal nevi, dysplastic nevi, primary melanoma and metastatic melanoma were performed using tissue microarray technique (Fig. 3-1). Moderate to strong NF-κB p105/p50 staining was recorded in 21% (3/14), 72% (37/51), 76% (142/185) and 78%

(43/55) in normal nevi, dysplastic nevi, primary melanoma and metastatic melanoma, respectively. While majority of normal nevi has negative to weak staining (79%), expression of NF-κB p105/p50 was significantly increased in dysplastic nevi, primary melanoma and metastatic melanoma compared to normal nevi (p=0.0004, χ^2 test) (Fig.3-2*A*). However, there is no significant difference in NF-κB p105/p50 staining between dysplastic nevi and primary melanoma (p=0.53, χ^2 test), or between primary melanoma and metastatic melanoma (p=0.83, χ^2 test) (Fig.3-2*A*). No association was observed between NF-κB p105/p50 overall expression with age, gender, subtype and location of tumors (Table 3-1).

Since nuclear translocation is required for the transcriptional activity of NF-κB, we assessed the percentage of cells showing positive NF-κB p105/p50 staining in nucleus. Strong NF-κB p105/p50 nuclear staining was recorded in 14, 45, 63, and 82% of normal nevi, dysplastic nevi, primary melanoma and metastatic melanoma biopsies, respectively (Fig. 3-2*B*). Significant differences in NF-κB p105/p50 nuclear staining were observed between normal nevi and dysplastic nevi (p=0.035, χ^2 test), between dysplastic nevi and primary melanoma (p=0.023, χ^2 test), and between primary melanoma and metastatic melanoma (p=0.008, χ^2 test) (Fig. 3-2*B*). In addition, no association was detected between NF-κB p105/p50 nuclear expressions with age, gender, subtype and location of tumors (Table 3-2).

3.2.3 Strong nuclear expression of NF-κB p105/p50 is inversely correlated with 5-year survival of patients with thick melanomas

Since tumor thickness is an important prognostic marker for melanoma, we divided the patients with primary melanoma into two subgroups: 1) low-risk group, thickness ≤2.0 mm; and 2) high-risk group, thickness >2.0 mm. To evaluate whether nuclear expression of NF-κB p105/p50 in human melanoma is correlated with a worse prognosis, Kaplan-Meier survival curves were plotted. We found that while nuclear NF-κB p105/p50 expression did not correlate with 5-year survival of patients with thin melanomas (≤2.0 mm) (p=0.82, log-rank test; Fig. 3-3*A*), strong NF-κB p105/p50 nuclear staining is significantly correlated with a poorer disease-specific 5-year survival of patients with thick melanomas (>2.0 mm) (p=0.014, log-rank test) (Fig. 3-3*B*). To further examine whether strong NF-κB p105/p50 nuclear staining is an independent prognostic marker for thick melanomas, we performed a multivariate analysis including p105/p50 nuclear staining, age, sex, tumor thickness, location and ulceration. Our result indicated that NF-κB p105/p50 nuclear staining reached a remarkable significance for predicting the patient outcome independent of other clinicopathologic parameters for 5-year disease-specific survival (Fig. 3-3*D*). We also evaluated the prognostic value of nuclear NF-κB expression in metastatic melanomas, but did not find a significant correlation (p=0.97, log-rank test; Fig. 3-3*C*).

3.3 Discussion

In the present study, we sought to determine the role of NF-κB p105/p50 in melanoma pathogenesis. Initially, we used TMA technology and immunohistochemistry to investigate the expression level of NF-κBp105/p50 in various stages of melanocytic lesions. Expression level of NF-κB subunit RelA has been well-studied in melanoma. NF-κB subunit RelA and serine-529 phosphorylated RelA has been shown to be overexpressed in melanoma biopsies (Shattuck-Brandt and Richmond 1997; McNulty, del Rosario et al. 2004). However, little is known of the expression level of NF-κB p105/p50 in melanoma. Our data demonstrated that the expression of NF-κB p105/p50 was significantly increased in dysplatic nevi, primary and metastatic melanoma comparing with normal nevi (Fig. 3-2*A*). In addition, we assessed the nuclear staining of NF-κB p105/p50 in melanoma biopsies since nuclear translocation of NF-κB subunits is one of critical steps for transcriptional activation of NF-κB. We have for the first time found that strong nuclear staining of NF-κB p105/p50 correlated with melanoma progression (Fig. 3-2*B*).

The progression of melanoma requires multiple genetic alterations. For example, we previously found that p-Akt expression is increased in melanoma compared with dysplastic nevi and inversely correlated with 5-year survival of patients with thin melanomas (Dai, Martinka et al. 2005). The expression of the small GTPase RhoC is related to metastatic phenotype of melanomas (Clark, Golub et al. 2000). In the present study, we found that nuclear staining of NF-κB p105/p50 is correlated with disease-specific 5-year survival of patients with thick melanomas (thickness >2.0 mm), and nuclear expression of NF-κB p105/p50 is an independent prognostic factor in patients with thick

melanomas (Fig. 3-3*B,D*). Our data suggest that increased nuclear expression of NF-κB p105/p50 is an important event during melanoma progression, possibly involved in the vertical growth phase.

Recent reports showed that NF-κB subunit p50 might be more important than other NF-κB subunits in the pathogenesis of classical Hodgkin lymphoma (Mathas, Johrens et al. 2005), nasopharyngeal carcinoma (Thornburg, Pathmanathan et al. 2003) and cervical carcinoma (Prusty, Husain et al. 2005). In addition, the expression level of IκBα, which retains NF-κB subunits in the cytoplasm and inhibits their nuclear translocation was higher in nevi than in melanoma biopsies (McNulty, del Rosario et al. 2004), Therefore, we speculate that increased expression of NF-κB RelA and p105/p50 occurs during melanoma development, but their transcriptional potential is inhibited by IκBα. During melanoma progression, the expression of IκBα is decreased, resulting in nuclear accumulation of NF-κB dimers and enhanced transcriptional activity.

In summary, our data demonstrated that NF-κB p105/p50 may be an important marker for human melanoma progression and prognosis.

3.4 Tables & Figures

Table 3-1 Overall expression of NF-κB p105/p50 and clinicopathological characteristics

	Expression of NF-κB p105/p50										Total	*P* Value[a]
	Negative		Weak		Moderate		Strong					
Primary melanoma												
Gender												
Male	7	(7%)	14	(13%)	39	(37%)	46	(43%)			106	*P*>0.05
Female	3	(4%)	19	(24%)	32	(41%)	25	(32%)			79	
Age												
≤57	4	(4%)	15	(17%)	36	(40%)	34	(38%)			89	*P*>0.05
>57	6	(6%)	18	(19%)	35	(36%)	37	(39%)			96	
Tumor thickness(mm)												
≤0.75	0	(0%)	11	(22%)	25	(51%)	13	(27%)			49	
0.76-1.5	3	(4%)	10	(15%)	29	(43%)	26	(38%)			68	*P*>0.05
1.51-4.0	4	(10%)	8	(19%)	11	(26%)	19	(45%)			42	
>4.0	3	(12%)	4	(15%)	6	(23%)	13	(50%)			26	
Ulceration												
Absent	7	(4%)	29	(18%)	67	(43%)	54	(34%)			157	*P*>0.05
Present	3	(11%)	4	(14%)	4	(14%)	17	(61%)			28	
Tumor subtype[b]												
SSM	0	(0%)	21	(27%)	31	(39%)	27	(34%)			79	
LMM	3	(12%)	3	(12%)	12	(48%)	7	(28%)			25	*P*>0.05
Other	7	(9%)	9	(11%)	28	(35%)	37	(46%)			81	
Site[c]												
Sun-protected	5	(Kashani-Sabet, Sagebiel et al.)	25	(17%)	57	(39%)	59	(40%)			146	*P*>0.05
Sun-exposed	5	(13%)	8	(21%)	14	(36%)	12	(31%)			39	
Metastatic melanoma												
Gender												
Male	4	(11%)	4	(11%)	9	(24%)	21	(55%)			38	*P*>0.05
Female	1	(6%)	3	(18%)	4	(24%)	9	(53%)			17	
Age												
≤57	2	(8%)	4	(15%)	10	(38%)	10	(38%)			26	*P*>0.05
>57	2	(7%)	4	(14%)	3	(10%)	20	(69%)			29	

[a] $\chi 2$ test for negative (1) to weak (2, 3) versus moderate (4, 5) to strong (6, 7) expression of NF-κB p105/p50.

[b] SSM, superficial spreading melanoma; LMM, lentigo maligna melanoma; Other includes desmoplastic melanoma, acrolentigous melanoma, and nodular melanoma.

[c] Sun-protected sites: trunk, arm, leg, and feet. Sun-exposed sites: head and neck.

Table 3-2 Nuclear expression of NF-κB p105/p50 and clinicopathological characteristics

	Nuclear expression of NF-κB p105/p50							
	Weak (≤50%)		Strong (>50%)		Total	*P* Value[a]
Primary melanoma						
Gender						
Male	39	(37%)	67	(63%)	106	*P*>0.05
Female	30	(38%)	49	(62%)	79	
Age						
≤57	38	(43%)	51	(57%)	89	*P*>0.05
>57	31	(32%)	65	(67%)	96	
Tumor thickness(mm)						
≤0.75	18	(37%)	31	(63%)	49	
0.76-1.5	24	(35%)	44	(65%)	68	*P*>0.05
1.51-4.0	18	(43%)	24	(57%)	42	
>4.0	9	(35%)	17	(65%)	26	
Ulceration						
Absent	57	(36%)	100	(64%)	157	*P*>0.05
Present	12	(43%)	16	(57%)	28	
Tumor subtype[b]						
SSM	29	(37%)	50	(63%)	79	
LMM	10	(40%)	15	(60%)	25	*P*>0.05
Other	21	(26%)	60	(74%)	81	
Site[c]						
Sun-protected	50	(34%)	96	(66%)	146	*P*>0.05
Sun-exposed	19	(49%)	20	(51%)	39	
Metastatic melanoma						
Gender						
Male	9	(24%)	29	(76%)	38	*P*>0.05
Female	5	(29%)	12	(71%)	17	
Age						
≤57	6	(23%)	20	(77%)	26	*P*>0.05
>57	6	(21%)	23	(79%)	29	

[a] $\chi 2$ test for weak versus strong nuclear expression NF-κB p105/p50.
[b] SSM, superficial spreading melanoma; LMM, lentigo maligna melanoma; Other includes desmoplastic melanoma, acrolentigous melanoma, and nodular melanoma.
[c] Sun-protected sites: trunk, arm, leg, and feet. Sun-exposed sites: head and neck.

Figure 3-1 Expression and localization of NF-κB p105/p50 in cutaneous melanoma tissue microarray. *A*, Normal nevus with weak staining. *B*, Dysplastic nevus with moderate staining. *C*, Primary melanoma with moderate staining. *D*, Metastastic melanoma with strong staining. Arrows indicate nuclear staining. Magnification, ×400.

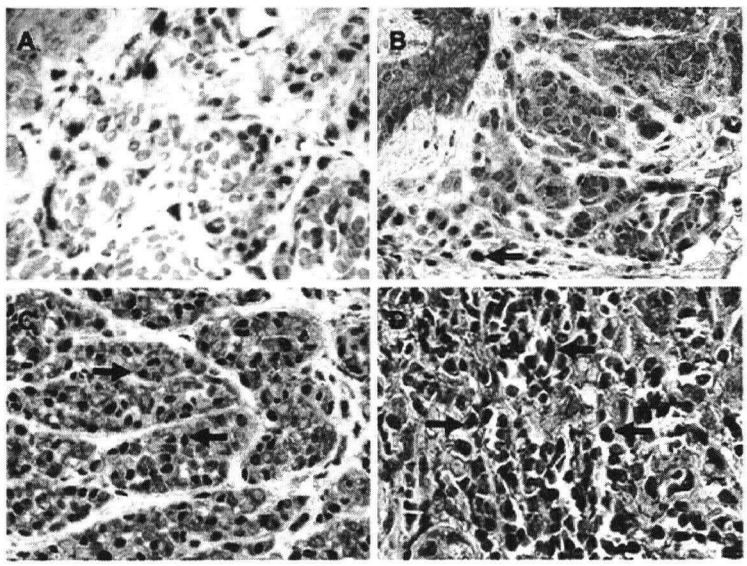

Figure 3-2 Expression of NF-κB p105/p50 and its nuclear localization in normal nevi (NN), dysplastic nevi (Eigentler, Caroli et al.), primary melanoma (PM) and metastatic melanoma (MM). *A*, Overall NF-κB p105/p50 expression is significantly increased in dysplastic nevi, primary melanoma and metastatic melanoma compared with normal nevi. *B*, Significant differences of nuclear staining of NF-κB p105/p50 were observed between normal nevi and dysplastic nevi (p=0.035, χ^2 test), between dysplastic nevi and primary melanoma (p=0.023, χ^2 test), between primary melanoma and metastatic melanoma (p=0.008, χ^2 test).

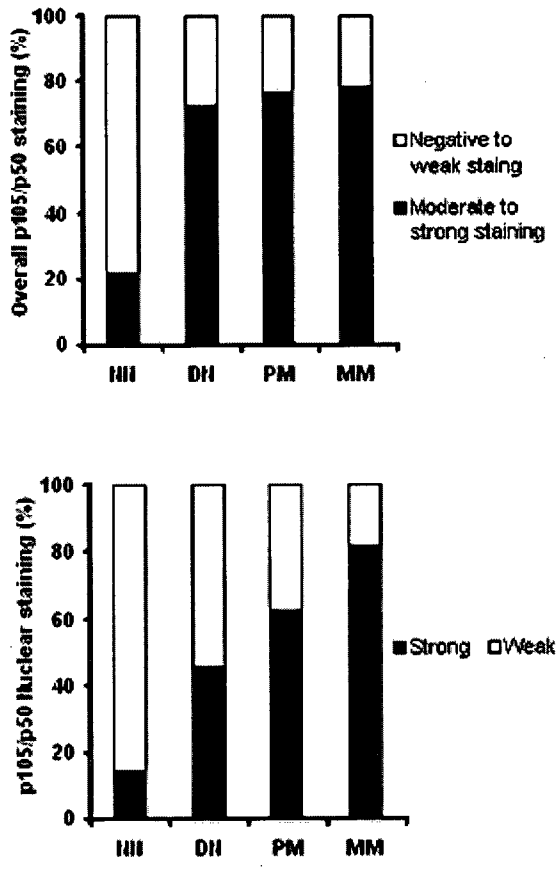

Figure 3-3 Prognostic value of NF-κB p105/p50 nuclear expression in subgroups of melanoma patients. *A*, Disease-specific 5-year survival of patients with thin melanoma (thickness ≤2.0 mm; p=0.82, log-rank test). *B*, Disease-specific 5-year survival of patients with thick melanomas (thickness >2.0 mm; p=0.014, log-rank test). *C*, Disease-specific 5-year survival of patients with metastatic melanomas (p=0.97, log-rank test). *D*, Multivariate Cox regression analysis of NF-κB p105/p50 nuclear expression with thick melanomas. *Coding of variables: NF-κB p105/p50 nuclear staining was coded as 1, weak expression; and 2, strong expression. Thickness was coded as 1, >2.0 mm, and 2, ≤2.0 mm. Ulceration was coded as 1, absent; and 2, present. Location was coded as 1, extremities and trunk; and 2, head and neck. Age was coded as 1, ≥ 57 years; and 2, <57 years. Sex was coded as 1, male; and 2, female.

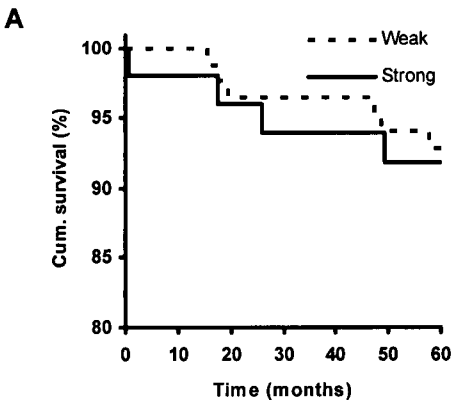

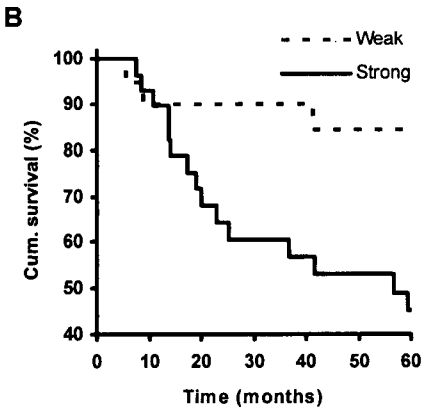

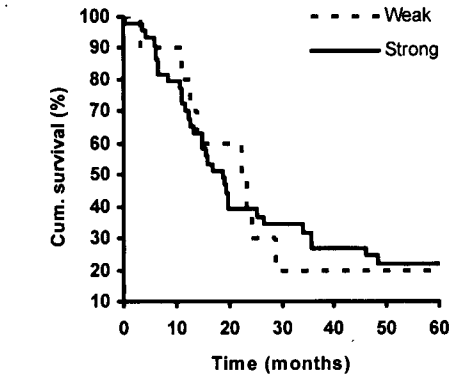

D

Variable*	Relative Risk	95 % CI	*p*
p105/50	4.177	1.057 - 14.424	0.041
Sex	0.671	0.243 - 1.788	0.413
Age	0.447	0.260 - 1.938	0.504
Thickness	1.310	0.198 - 1.530	0.252
Location	2.998	0.890 - 6.620	0.083
Ulceration	2.294	0.798 - 5.823	0.130

Chapter 4. Nuclear factor kappaB subunit p50 promotes melanoma cell migration

4.1 Rationale

The progression of melanoma from radical growth phase to vertical growth phase was accompanied by acquisition of metastatic potential (Gray-Schopfer, Wellbrock et al. 2007). Classically the dynamics of tumor cell metastasis consists of local invasion, intravasation and finally colonization in the new sites, which require tumor cell become motile, degrade matrix and penetrate stromal cells (Labrousse, Ntayi et al. 2004; Ara and DeClerck 2006).

High NF-κB activity has been shown to be involved in tumor metastasis. The constitutively active NF-κB plays a major role in the production of chemokines such as CXCL1 and CXCL8 (Kunz, Hartmann et al. 1999; Yang and Richmond 2001). In addition, GTPases (RhoA, cdc42 and Rac1), which are key regulators of cell motility, phosphorylate IκB and translocate p65/p50 or p50/p50 dimers to the nucleus, promoting stress fiber formation and cell migration (Perona, Montaner et al. 1997; Montaner, Perona et al. 1998; Jimenez, Portela et al. 2000)

Since our TMA data showed that increased NF-kB expression is associated with thick melanoma, it suggested NF-kB expression may be correlated with vertical growth phase, which renders melanoma cells becoming motile. Therefore, we postulated NF-kB p50 may play an important role in melanoma cell migration.

4.2 Results

4.2.1 NF-κB p50 promotes melanoma cell migration

Since cell migration is one of the central steps of cancer metastasis that greatly shortens the survival of melanoma patients, we investigated the involvement of NF-κB p50 in melanoma cell migration. We first transiently transfected MMRU and Sk-mel-3 melanoma cells with pCMV-hp-p50 expression vector or control pCMV vector. Cells were harvest at 24, 48, and 72 h after transfection and extracts were analyzed by Western blot. The maximal level of NF-κB p50 expression was observed at 24 h after transfection and the increased level of NF-κB p50 lasted up to 72 h (Fig . 4-1*A*) in MMRU melanoma cells and 48 h (Fig. 4-1B) in Sk-mel-3 melanoma cells, respectively. Wound healing assay was performed after the transfected cells were incubated with 10 μg/ml mitomycin C for 2 h, which inhibits cell division, so that the difference in cell motility was not due to the differences in cell proliferation. MMRU and Sk-mel-3 melanoma cells transfected with NF-κB p50 almost healed the wound 12 or 24 h after scratch, while the cells transfected with vector were unable to heal the wound at the same time point (Fig. 4-1*C*). Overexpression of NF-κB p50 resulted in more than two-fold migrated cells in wound area compared with vector controls (Fig. 4-1*C*).

4.2.2 Silencing of NF-κB p50 inhibits melanoma cell migration

To test whether a physiological level of NF-κB p50 plays a role in melanoma cell migration, we used siRNA to knockdown NF-κB p105, the precursor of NF-κB p50 in MMRU melanoma cells. Fig. 4-2*A* depicts the efficiency of the siRNA transfection as measured by Western blot analysis. Accompanied with

more than 90% downregulation of NF-κB p105 expression level, the level of NF-κB p50 also gradually decreased from 24 to 72 h after transfection. Wound healing assay was performed 24 h after transfection. Migration ability of cells transfected with NF-κB p105 siRNA was significantly reduced whereas cells transfected with control siRNA almost closed the wound 20 h after the wounds were introduced (Fig. 4-2*B*). NF-κB p105 siRNA reduced the number of migrated cells by 2-fold compared with the control siRNA (Fig. 4-2*C*)

4.2.3 NF-κB p50 enhances RhoA activity and stress fiber formation via Rock

It is well-established that RhoA-Rock pathway plays an important role in cell migration through reorganization of stress fiber(Maekawa, Ishizaki et al. 1999). To address whether changes of NF-κB p50-transfected cell migration were related to *in vivo* level of active RhoA, RhoA pull-down assay was performed. Cells were transfected with pCMV-hp50 or pCMV vector, or without transfection as control. Then all the cells were serum-starved for 24 h and RhoA activity was induced by serum stimulation of transfected cells for 3 min. Fig. 4-3*A* shows that RhoA activity is undetectable or very low in untransfected or pCMV vector transfected control cells, while the RhoA activity is greatly induced in cells transfected with NF-κB p50. Moreover, serum-induced formation of stress fiber is more excessive in MMRU cells transfected with NF-κB p50 than those with vector control after 30 min of serum stimulation (Fig. 4-3*B)*, while Rock inhibitor, Y27632, effectively abrogated the regulatory function of NF-κB p50 in stress fiber formation (Fig. 4-3*C)*.

4.3. Discussion

Cell migration is one of the critical steps for tumor invasion and progression (Hendrix, Seftor et al. 2003). Our *in vitro* data by overexpressing NF-κB p50 (Fig. 4-1) and treatment with p105 siRNA (Fig. 4-2) clearly demonstrated that this subunit is crucial for the motility of melanoma cells. The process of cell migration is related to the network of various types of extrocellular growth factors, chemokines, transmembrane receptors and intracellular factors (Ridley, Schwartz et al. 2003; Gassmann, Enns et al. 2004; Suyama, Kawasaki et al. 2004). Since nuclear NF-κB can lead to enhanced gene transcription, its role in melanoma cell migration is most likely associated with the activation of its downstream targets. It is well known that Rho GTPase family proteins are essential elements to regulate cell shape, polarity and locomotion (Horwitz and Webb 2003). Rho proteins are activated when bound to GTP and are inactivated upon hydrolysis of GTP to GDP (Jaffe and Hall 2005). Three main families regulate their activity, guanine nucleotide exchange factors (GEFs) that catalyze exchange of GDP to GTP, GTPase-activating proteins (GAPs) that stimulate hydrolyze GTP to GDP, and guanine nucleotide dissociation inhibitors (GDIs) that appears to block the spontaneous activation (Hall 1998; Ren, Kiosses et al. 1999; Schmidt and Hall 2002). RhoA, Rac 1 and Cdc42 are three well-studied members of Rho family, all of which are pivotal regulators of reorganization of actin during cell migration (Burridge and Wennerberg 2004; Wheeler and Ridley 2004). Therefore, it is possible that NF-κB p50 may activate RhoA to induce cell migration through regulation of actin organization. The results from RhoA pull-down assay indeed indicate that RhoA activity is dramatically enhanced in

cells transfected with NF-κB p50 compared with vector control (Fig. 4-3*A*). We also investigated the effect of NF-κB p50 on the activity of Rac1 and cdc42, but no significant difference in Rac1 or cdc42 activity was found between melanoma cells transfected with NF-κB p50 and vector control (data not shown). Furthermore, our findings provided evidence that overexpression of NF-κB p50 resulted in enhanced stress fiber formation, while Rock inhibitor, Y27632, can inhibit this effect, which confirmed the regulatory role of NF-κB p50 in RhoA-Rock pathway.

On the other hand, previous study suggested that NF-κB could be activated by RhoA, Cdc42 and Rac1 (Perona, Montaner et al. 1997). These Rho proteins induced phosphorylation of IκB and translocation of p50/p50 and p50/p65 dimers to the nucleus. Therefore, we speculate that NF-κB p50 serves as a positive feedback factor to RhoA activity.

In summary, we demonstrated that elevated activity of NF-κB p105/p50 may facilitate tumor progression by enhancing cell migration and RhoA activity as well as stress fiber formation via Rock.

4.4 Figures

Figure 4-1 Overexpression of NF-κB p50 promotes melanoma cell migration and RhoA activity. *A*, MMRU and Sk-mel-3 melanoma cells were transfected with NF-κB p50 or control vector and extracts of the cells were analyzed for the expression of NF-κB p50 by Western blot analysis. *B*, Wound healing assay was performed on monolayers of MMRU (upper panel) and Sk-mel-3 (lower panel) melanoma cells after 24 h transfection. The photographs of MMRU and Sk-mel-3 melanoma cells were taken at 12 and 24 h respectively after wounds were made. *C*, Quantitation of *B*. The number of migrating MMRU and Sk-mel-3 cells transfected with NF-κB p50 were 2-fold higher than cells transfected with vector. Each value represents the mean $\pm$ SD of triplicates. Similar results were observed in three independent experiments. Magnification, ×100.

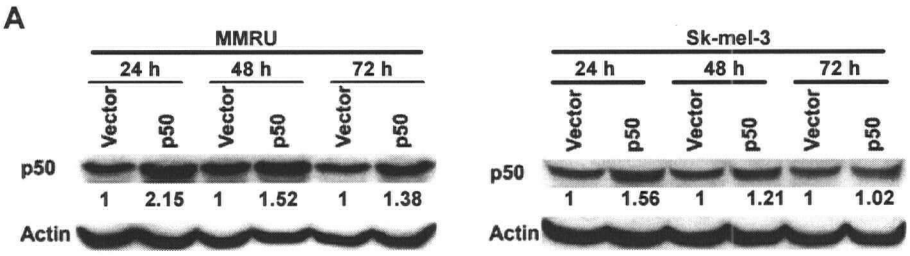
A
MMRU
24 h
48 h
72 h
Vector
p50
Vector
p50
Vector
p50
p50
1
2.15
1
1.52
1
1.38
Actin
Sk-mel-3
24 h
48 h
72 h
Vector
p50
Vector
p50
Vector
p50
p50
1
1.56
1
1.21
1
1.02
Actin

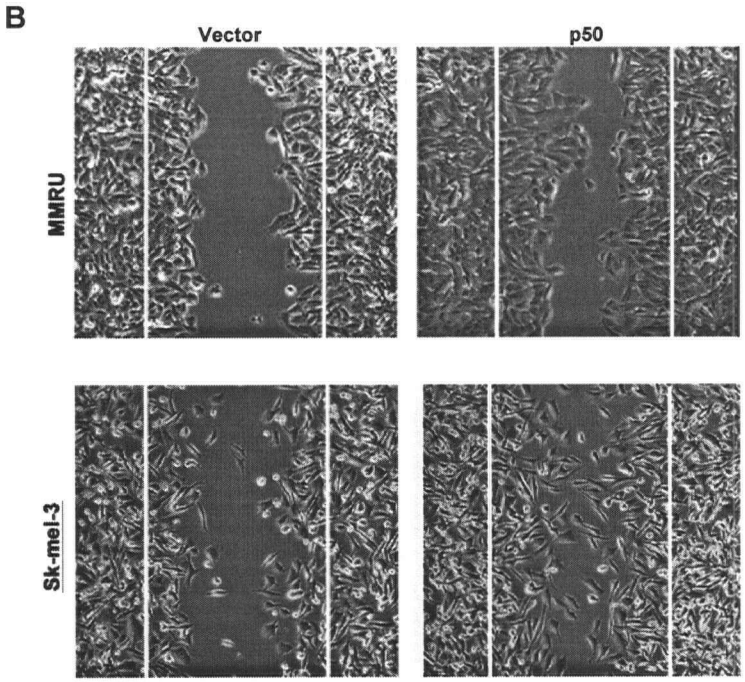
B
Vector
p50
MMRU
Sk-mel-3

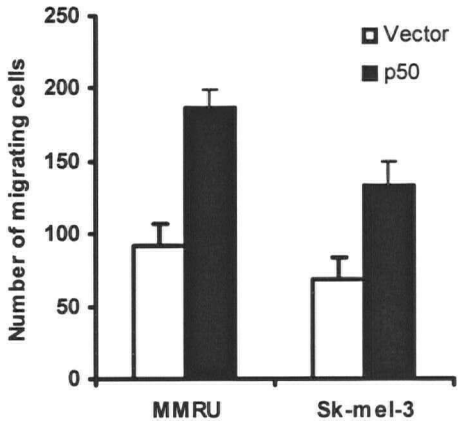
C
Number of migrating cells
250
200
150
100
50
0
Vector
p50
MMRU
Sk-mel-3

Figure 4-2 Downregulation of NF-κB p50 inhibits melanoma cell migration. *A*, MMRU melanoma cells were transfected with NF-κB p105 siRNA or control siRNA. Western blot assay was performed to measure the expression level of NF-κB p105/p50 and actin at 24, 48 and 72 h after transfection. *B*, The monolayer of MMRU melanoma cells was scratched 24 h after transfection and photographed 20 h later. *C*, Quantitation of *B*. The number of migrating cells transfected with NF-κB p105 siRNA were 50% less than those transfected with control siRNA.

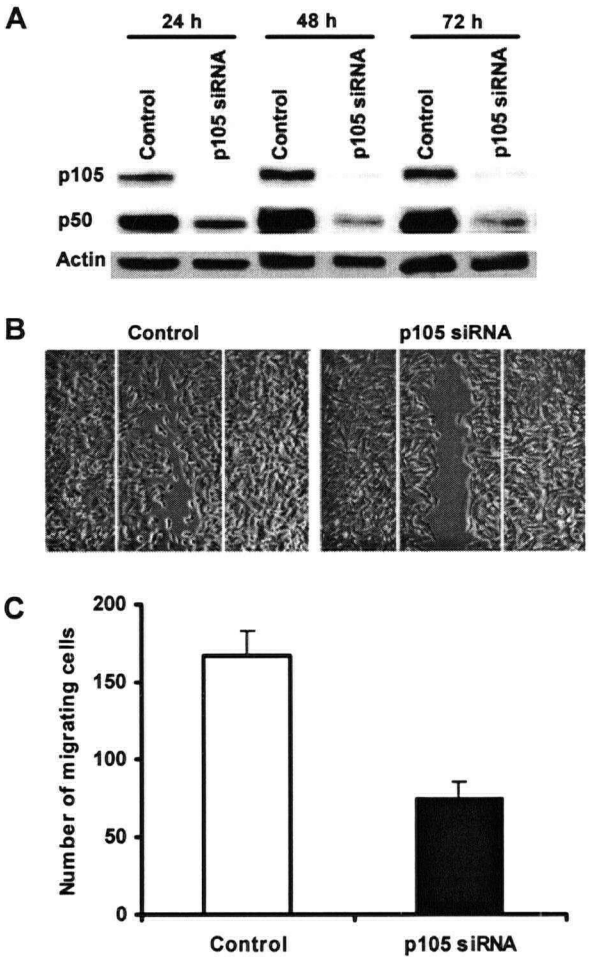

Figure 4-3 NF-κB p50 enhances RhoA activity and stress fiber formation via Rock. *A*, NF-κB p50 enhances RhoA activity determined by RhoA pull-down assay. Lane 1, MMRU cells without transfection were serum-starved for 24 h. Lanes 2 and 3, MMRU cells were transfected with pCMV vector or pCMV-hp50, respectively, followed by serum-starvation for 24 h and serum stimulation for 3 min. *B* and *C,* NF-κB p50 enhances stress fiber formation mediated by Rock. Cells were transfected with pCMV vector or pCMV-hp50, respectively, followed by serum-starvation overnight and serum stimulation. *B,* Cells transfected with NF-κB p50 display more stress fibers than cells transfected with vector after serum stimulation 30 min. *C,* Cells were pre-treated with serum-free medium with 10 μM Y27632 for 2 h after transfection with pCMV vector or pCMV-hp50 and serum-starvation overnight, and then incubated with complete medium containing 10% FBS and 10 μM Y27632 for 30 min.

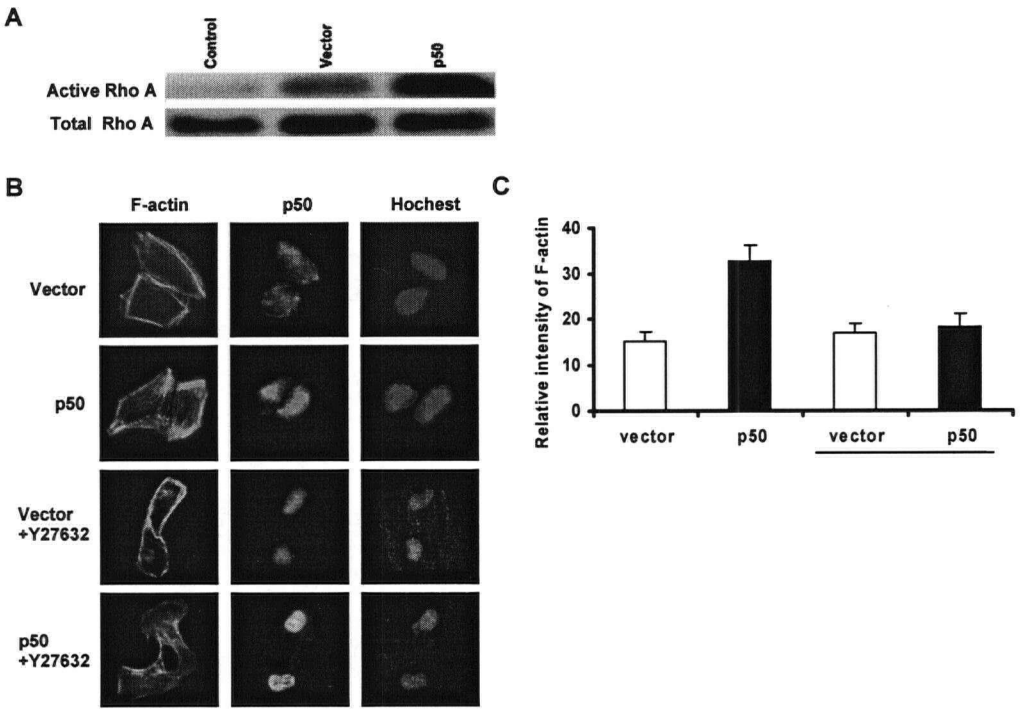

Chapter 5. Nuclear factor kappaB subunit p50 promotes melanoma angiogenesis via upregulating interleukin-6 expression

5.1 Rationale

Since the earliest days of tumor angiogenesis research melanoma is well-known for its active formation of new blood vessels (Warren and Shubik 1966). Angiogenesis is a process involving the growth of new blood vessels, which is essential for tumor growth, invasion and metastasis (Hanahan and Weinberg 2000). Using tissue microarray technology, a prospective study of 417 cutaneous melanoma revealed that the most important determinant of overall survival is tumor vascularity, suggesting the important role of angiogenesis in melanoma progression (Kashani-Sabet, Sagebiel et al. 2002). A few antiangiogenic agents have been applied in phase I to III clinical trial of melanoma patients (Sosman and Puzanov 2006).

However, application of single antiangiogenesis reagent lacks of antitumor efficacy because cancer cells release a number of different proangiogenic factors which easily bypass such specific targets. The desired treatment would be a combination of a few antiangiogenic agents and traditional chemotherapy or to target the common upstream of proangiogenic cytokines (Streit and Detmar 2003). Therefore NF-κB is of increasing interest due to its important role in angiogenesis by promoting several factors such as VEGF, IL-1 and IL-8 in addition to its role in tumor growth, antiapoptosis and metastasis. But complete inhibition of NF-κB may cause severe side effects because the activity of NF-κB is required for maintain normal immunity and hematopoiesis (Aggarwal 2004). Lack of selective blockade of NF-κB activity

is due to the poor understanding of specific functions of NF-κB family members in different cell types. In this study we identified that *IL-6* expression was highly induced by overexpression of NF-κB subunit p50 using cDNA microarray technology. Since IL-6 is a newly reported proangiogenic factor in cancer, we hypothesized that NF-κB p50 could promote melanoma angiogenesis by upregulating IL-6.

5.2 Results

5.2.1 Overexpression of NF-κB subunit p50 does not change the growth rate of MMRU melanoma cells

To identify the direct downstream targets of NF-κB p50, MMRU melanoma cell was transfected with expression vector pCMV or pCMV-hp50. Clones stably expressing NF-κB p50 were selected with G418. The expression of NF-κB p50 in stable clones was evaluated by Western blot. The clone M6 and M8 have higher expression of NF-κB p50 compared with vector clone (Fig. 5-1*A*). However, these clones only show marginal differences in their growth rates (Fig. 5-1*B*).

5.2.2 Gene expression profile regulated by NF-κB p50 in MMRU melanoma cells

To assess the globe effects of NF-κB p50 in melanoma cells, we performed the expression analysis of 21,000 genes in p50-overexpressing clone M8 and vector clone by cDNA microarray. Clone M8 was chose due to its high p50 expression determined by Western blot (Fig. 5-1*A*). cDNA mircroarray analysis identified 179 genes which were significantly altered (≥2 fold) in M8 clone compared with vector clone (Fig. 5-2 and table 5-1). The gene with the highest fold change is *IL-6*, which is induced 15 times by NF-κB p50.

5.2.3 Validation of gene expression profiles by real-time RT-PCR

To examine the reliability of the expression changes identified by cDNA microarray analysis, the top 5 genes induced or inhibited by NF-κB p50 (*IL-6, VIP-R-1, SLC14A1, IL-1A, Megsin, NGAL, S100B, SULF1, TRIM9 and*

MYBPC1) were selected for real-time RT-PCR analysis. Fold changes obtained from quantitative RT-PCR were in agreement with cDNA microarray data (Fig. 5-3).

5.2.4 NF-κB p50 promotes angiogenesis *in vitro* and *in vivo*

Considering the pro-angiogenic role of IL-6 in cancer, we, therefore, investigated if NF-κB p50 is involved in angiogenesis by upregulating IL-6. IL-6 concentration induced by p50 was determined by ELISA. Fig. 5-4*A* shows that the level of IL-6 in p50-overexpressing clone M8 is almost 5 times higher than that of vector clone. The upregulation of IL-6 by NF-κB p50 was also observed in another p50-overexpressing clone M6. Conditioned medium from clone M8 stimulated the proliferation of HUVECs compared with conditioned medium from vector clone. When IL-6 antibody (2 μg/ml; Propetech, NJ) was added to neutralize IL-6, it abrogated the effect of the conditioned medium from clone M8 (Fig. 5-4*B*). In addition, matrigel plug assay demonstrated that p50-overexpressing clone dramatically induced more vascularization than vector clone (Fig. 5-4*C*). To further support that NF-κB p50 induced melanoma angiogenesis, we compared the hemoglobin level between matrigel plugs from vector and M8 clones and found that hemoglobin level was clearly elevated in plugs containing p50-overexpressing cells (P=0.01, student t-test) (Fig. 5-4*D*).

5.2.5 Silence of NF-κB p50 inhibits IL-6 expression in MMRU melanoma cells

To assess if a physiological level of NF-κB p50 plays a role in IL-6 production, we used shRNA to knock-down NF-κB p105, the precursor of NF-κB p50 in

MMRU melanoma cells. Figure 5-5*A* depicts that expression of p105 and p50, but not p65, was clearly inhibited by p105 shRNA as measured by Western blot analysis. The mRNA level and protein level of IL-6 were also decreased after p105 shRNA treatment, confirming that NF-κB regulates IL-6 expression at the transcriptional level (Fig. 5-5*B* and *C*).

Since AFT3 can interact with Rel to regulate IL-6 expression in macrophage (Gilchrist, Thorsson et al. 2006), we examined if ATF3 can antagonize the induction of IL-6 by NF-κB p50. We cotransfected ATF3 and p50 into MMRU melanoma cells and found that ATF3 can abrogate the effect of p50 on induction of IL-6 24 h after transfection as measured by conventional PT-PCR and ELISA (Fig. 5-5*D* and *E*).

5.3 Discussion

Despite the complexity of NF-κB family, the specific function of its members (p65/RelA, RelB, c-Rel, p105/p50 and p100/p52) is of increasing interest to the scientific community because of their potential significance for targeted therapy. Overexpression of RelA inhibits TRAIL-induced apoptosis in breast cancer cells (Chen, Kandasamy et al. 2003). p100/52 directly regulates expression of cyclin D1 and p53-target genes in osteosarcoma cells (Schumm, Rocha et al. 2006). Constitutive *de novo* synthesis of RelB is active in estrogen receptor alpha (ERα)-negative breast cancer cells and contributes to their invasive phenotype (Wang, Belguise et al. 2007). In the present study, we demonstrated that NF-κB p50 is essential for IL-6 expression in human MMRU melanoma cells. Overexpression of NF-κB p50 highly induced IL-6 expression (Table 5-1, Fig. 5-2, 5-3) while the level of IL-6 was decreased after knockdown of p105/p50 (Fig. 5-5). In addition, we showed that NF-κB p50 promoted angiogenesis *in vitro* and *in vivo*.

IL-6 is a multi-functional factor in cancer pathogenesis, which is involved in anti-apoptosis, proliferation and chemoresistance (Culig, Steiner et al. 2005; Cavarretta, Neuwirt et al. 2006; Domingo-Domenech, Oliva et al. 2006; Nicolini, Carpi et al. 2006). In melanoma, serum level of IL-6 was significantly increased in patients with metastatic melanoma and correlated with poor survival. It has demonstrated that IL-6 activated a few pathways such as JAK/STAT3, PI3 kinase/AKT and MAPK pathways (Huang, Wu et al. 2004; Jee, Chu et al. 2004; Meng, Yamagiwa et al. 2005) in cancer cells. Recent studies also revealed that IL-6 played an important role in angiogenesis through inducing endothelial cell migration and proliferation

(Nilsson, Langley et al. 2005; Yao, Zhai et al. 2006). In agreement with these findings, our data showed that conditioned medium from p50-overexpressing clone, which contains high concentration of IL-6, stimulated the proliferation of HUVECs while IL-6 antibody neutralized IL-6 in the conditioned medium and abrogated the effect of IL-6 on HUVECs proliferation (Fig. 5-4*B*). *In vivo* angiogenesis assay confirmed that p50 enhanced vascularization similarly as IL-6 (Fig. 5-4*C*, *D*) (Nilsson, Langley et al. 2005).

Although the expression of numerous cytokines including IL-6 was regulated by activities of NF-κB, their functions seem to be tightly controlled by the structure of NF-κB family members, the promoter sequences of target genes, as well as coactivators or inhibitors(Ghosh, May et al. 1998; Leung, Hoffmann et al. 2004; Gilchrist, Thorsson et al. 2006). For example, p50 homodimer forms a complex with co-activator CREB-binding protein activating the transcription of IL-10. Macrophages from p50-/- mice decreased IL-10 production and increased expression of IL-12 and tumor necrosis factor upon LPS stimulation (Cao, Zhang et al. 2006). Another recent study predicted that the interaction of p105/p50 with ATF3 may affect the expression of IL-6 in macrophage (Gilchrist, Thorsson et al. 2006). We then postulate that AFT3 would be an inhibitor of p50 function. Indeed, overexpression of ATF3 decreased the IL-6 expression induced by p50 (Fig. 5-5*D*, *E*). It implied that similar mechanism of ATF3 downregulating IL-6 expression exists in MMRU melanoma cells.

Our previous data showed that overexpression of p50 enhanced the melanoma cell migration (Gao, Dai et al. 2006). However, neither recombinant IL-6 nor ovexexpression of IL-6 in MMRU melanoma cells can increase the

cell motility (data not shown), suggesting that IL-6 is not involved in melanoma cell migration.

In summary, we demonstrated that NF-κB p50 specifically induced IL-6 expression, resulting enhanced angiogenesis in vitro and in vivo while knockdown of p105/p50 greatly interfered with IL-6 expression. In addition, our previous data have shown that p105/p50 is an important marker for the prognosis of melanoma patients and p50 promoted cell migration through activating RhoA (Gao, Dai et al. 2006). Therefore, NF-κB p105/p50 would be a potential therapeutic target for human melanoma.

5.4 Tables and figures

Table 5-1 179 differentially expressed genes in NF-κB p50-overexpressing clone M8 compared with vector clone

Probe ID	Known gene name	p value	Fold change
H200010620	Interleukin-6 (IL-6)	0.0006	15.1
H200020274	Vasoactive intestinal polypeptide receptor 1	0.0013	10.2
H200007987	SLC14A1	0.0144	7.89
H200000451	Interleukin-1 alpha(IL-1 alpha)	0.0271	7.61
H200013276	Megsin	0.0328	6.72
H200014828	Protein MICAL-2	0.0054	5.66
H200016225	APOBEC3G	0.0189	5.59
H200016159	Transcription factor 19	0.0367	5.56
H200011805	Normal mucosa of esophagus specific gene 1 protein	0.0369	5.32
H200012604		0.0017	5.31
H200004964		0.0056	5.17
H200019450		0.0060	5.05
H200012985	cardiotrophin-like cytokine	0.0283	4.75
H200016773	Integrin alpha-2 precursor	0.0055	4.62
H200008209	neuron navigator 3	0.0182	4.48
H200010451		0.0067	3.86
H200004451	S100 calcium-binding protein A2	0.0130	3.71
H200001031	Synaptopodin	0.0031	3.57
H200002766	Probable ubiquitin carboxyl-terminal hydrolase CYLD	0.0124	3.46
H200008438	Unc-112 related protein 1	0.0015	3.43
H200013648	Smoothelin	0.0002	3.36
H200001630	Protein-glutamine gamma-glutamyltransferase	0.0055	3.32
H200007979	Ephrin type-A receptor 2 precursor	0.0148	3.31
H200001892	CD166 antigen precursor	0.0030	3.29
H200011012	Tumor necrosis factor ligand superfamily member 7	0.0310	3.21
H200002394		0.0459	3.20
H200020254	intermediate filament protein syncoilin	0.0041	3.11
H200013413	Low-density lipoprotein receptor-related protein 3	0.0013	3.01
H200008365	Cyclin-dependent kinase inhibitor 1 (p21)	0.0004	2.99
H200004941	Leupaxin.	0.0105	2.97
H200002230	Lymphocyte specific adapter protein Lnk	0.0042	2.95
H200003337	Keratin, type II cytoskeletal 7	0.0117	2.95
H200013959	Fibroblast growth factor-20	0.0214	2.92
H200009616		0.0080	2.76
H200008363	Urokinase plasminogen activator surface receptor	0.0368	2.74

H200002718	amino acid transporter system A1	0.0210	2.72
H200000253	Natural killer cells protein 4 precursor	0.0054	2.70
H200011441		0.0439	2.70
H200009647	Tissue factor pathway inhibitor 2 precursor (TFPI-2)	0.0216	2.64
H200006072	Ribonucleoside-diphosphate reductase M2 chain	0.0071	2.63
H200007562	Numb protein homolog	0.0060	2.62
H200000264		0.0258	2.61
H200008377		0.0377	2.59
H200020138		0.0396	2.59
H200000265	Vitamin K-dependent protein Z precursor	0.0133	2.57
H200005768		0.0075	2.56
H200008789	mitochondrial ribosomal protein S24	0.0056	2.53
H200002641	Protein-tyrosine sulfotransferase 1	0.0004	2.49
H200020015		0.0134	2.49
H200011394		0.0328	2.48
H200007011	Interstitial collagenase precursor	0.0088	2.47
H200007725	Atrial natriuretic peptide receptor A precursor	0.0332	2.45
H200013798	Mitogen-activated protein kinase kinase kinase 5	0.0254	2.43
H200001880	Tumor necrosis factor receptor superfamily member Fn14	0.0027	2.41
H200016556	Integrin alpha-3 precursor	0.0047	2.39
H200005863	Vascular endothelial growth factor A precursor	0.0021	2.37
H200004003	G1/S-Specific cyclin E2	0.0405	2.36
H200001697	CYR61 protein precursor	0.0071	2.34
H200006989	G1/S-specific cyclin D1	0.0011	2.34
H200009948	Fat-specific protein FSP27 homolog	0.0385	2.34
H200009591		0.0452	2.32
H200015006	related RAS viral (r-ras) oncogene homolog 2	0.0122	2.28
H200009934	S100 calcium-binding protein A16	0.0054	2.27
H200007438	intimal thickness-related receptor	0.0044	2.26
H200011636	Nef-associated factor 1	0.0062	2.25
H200006805	DNA polymerase gamma subunit 1	0.0479	2.24
H200009351		0.0193	2.23
H200002747		0.0009	2.22
H200016224	NKG2D ligand 2 precursor	0.0131	2.22
H200006754	Keratin, type I cytoskeletal 15	0.0344	2.22
H200003873	Cell division cycle 7-related protein kinase	0.0082	2.21
H200009668		0.0140	2.20
H200020163	Putative HIF-prolyl hydroxylase PH-4	0.0224	2.16
H200003655	Transmembrane 4 superfamily member 7 (Novel antigen 2)	0.0097	2.15
H200014627	Smad ubiquitination regulatory factor 2	0.0112	2.15
H200007997	Poliovirus receptor precursor	0.0014	2.14

H200013928	pleckstrin homology-like domain family A member 2	0.0011	2.14
H200007065	Cytochrome b5	0.0021	2.10
H200001239		0.0204	2.10
H200004832		0.0226	2.08
H200005879	Bone morphogenetic protein 2 precursor (BMP-2) (BMP-2A).	0.0329	2.08
H200006069	Aldose reductase	0.0019	2.08
H200011606	Collagen alpha 1(Domingo-Domenech, Oliva et al.) chain precursor	0.0036	2.08
H200007050	Rho GDP-dissociation inhibitor 2	0.0320	2.07
H200005065	Vacuolar protein sorting 13A (Chorein)	0.0424	2.04
H200011786	SET binding factor 1	0.0393	2.04
H200017722	Carboxypeptidase A6 precursor	0.0138	2.03
H200018928		0.0147	2.03
H200004256	Cell division cycle associated protein 4	0.0400	2.01
H200006120	Connective tissue growth factor precursor	0.0268	2.00
H200011490	Latrophilin 1 precursor	0.0009	0.50
H200003924		0.0115	0.50
H200008568	POU domain, class 2, transcription factor 1	0.0143	0.50
H200015843		0.0029	0.50
H200005932	Aldehyde dehydrogenase family 7 member A1	0.0052	0.49
H200017492	calcium/calmodulin-dependent protein kinase ID	0.0360	0.49
H200006909	Semaphorin 3B precursor	0.0163	0.49
H200013933	Lipopolysaccharide-binding protein precursor (LBP)	0.0156	0.49
H200004493		0.0160	0.48
H200001987	chondroitin beta1,4 N-acetylgalactosaminyltransferase	0.0027	0.48
H200020576	Mas-related G-protein coupled receptor member X3	0.0163	0.48
H200018683		0.0202	0.48
H200001527		0.0237	0.47
H200004014		0.0207	0.47
H200011538	Sodium- and chloride-dependent transporter XTRP3	0.0402	0.47
H200014523	protein phosphatase 1	0.0258	0.47
H200010402	Pyruvate carboxylase, mitochondrial precursor	0.0250	0.46
H200004468	Integrin alpha-4 precursor	0.0243	0.46
H200006870	Polycystin 2	0.0065	0.46
H200018060	Prostacyclin synthase	0.0311	0.46
H200001150	arrestin domain containing 4	0.0126	0.46
H200019523	Ghrelin precursor	0.0449	0.46
H200014839	Receptor protein-tyrosine kinase erbB-3 precursor	0.0006	0.46

H200006348	Sodium/potassium-transporting ATPase beta-3 chain	0.0001	0.46
H200004179		0.0370	0.46
H200013135	Urocortin precursor	0.0065	0.45
H200000972	Formin binding protein 2 (srGAP2)	0.0418	0.45
H200013730	Fucose-1-phosphate guanylyltransferase	0.0315	0.45
H200001712		0.0010	0.44
H200015190	Laminin gamma-1 chain precursor (Laminin B2 chain)	0.0069	0.44
H200000021	Zinc-alpha-2-glycoprotein precursor	0.0320	0.44
H200003440		0.0187	0.44
H200005214	Insulin-induced protein 1.	0.0304	0.43
H200003487	GPI deacylase	0.0152	0.43
H200016671		0.0087	0.42
H200008291		0.0434	0.42
H200000621	Angiopoietin-1 precursor (ANG-1).	0.0036	0.41
H200020855		0.0240	0.41
H200006658	lipoma HMGIC fusion partner-like 2	0.0154	0.39
H200007274		0.0227	0.39
H200006744	RNA-binding protein with multiple splicing	0.0244	0.39
H200004873	Tumor necrosis factor receptor superfamily member 19 precursor	0.0347	0.39
H200008549	Glutamate receptor, ionotropic kainate 1 precursor	0.0074	0.39
H200017417	Matrix Gla-protein precursor	0.0306	0.39
H200006258	Decorin precursor	0.0200	0.39
H200020667		0.0388	0.38
H200006882	Cbp/p300-interacting transactivator 2	0.0325	0.37
H200014435		0.0474	0.37
H200001979	Autophagy protein 5-like (APG5-like)	0.0448	0.36
H200005990	MARCKS-related protein	0.0145	0.35
H200009209		0.0143	0.35
H200014019	B-cell lymphoma 6 protein	0.0436	0.35
H200003394		0.0076	0.35
H200006603	OX-2 membrane glycoprotein precursor	0.0026	0.34
H200008450	Scavenger receptor class B member 1	0.0188	0.33
H200016567	Fc receptor homolog expressed in B cells	0.0246	0.33
H200018140	Sulfate transporter	0.0192	0.33
H200006831	S100 calcium-binding protein A4	0.0004	0.33
H200006854	Versican core protein precursor	0.0074	0.32
H200016273		0.0096	0.31
H200006597	Myocyte-specific enhancer factor 2C.	0.0028	0.31
H200002118		0.0022	0.31
H200017874	Oxysterol binding protein-related protein 10	0.0395	0.31
H200010223	Transcription factor SOX-5	0.0156	0.30
H200007312	Syndecan-3 (SYND3).	0.0021	0.28
H200001575		0.0423	0.28
H200009536	S-100 protein, alpha chain	0.0146	0.28
H200009248	SLIT and NTRK-like protein 6	0.0201	0.27

H200001272	Breast carcinoma amplified sequence 3	0.0006	0.27
H200006318		0.0282	0.25
H200019015	T-box transcription factor TBX2	0.0013	0.25
H200001295	Guanine nucleotide-binding protein gamma-7 subunit.	0.0195	0.25
H200010192	Endothelin B receptor precursor	0.0128	0.25
H200012768	Alpha-methylacyl-CoA racemase	0.0122	0.25
H200003992		0.0046	0.24
H200006197	NDRG1 protein	0.0095	0.24
H200003683	Fatty acid-binding protein, brain (B-FABP)	0.0031	0.22
H200000350	Colipase precursor	0.0216	0.22
H200006566	Receptor-type protein-tyrosine phosphatase zeta	0.0067	0.21
H200013940	Chitinase 3-like protein 2 precursor	0.0247	0.20
H200005066	Collagen alpha 3(IX) chain precursor.	0.0040	0.19
H200005298	Scavenger receptor class F member 2 precursor	0.0256	0.19
H200018207	Aldo-keto reductase family 1 member C1	0.0224	0.17
H200007868	Myosin-binding protein C, slow-type	0.0413	0.16
H200005999	Tripartite motif-containing protein 9	0.0232	0.14
H200005722	Extracellular sulfatase Sulf-1	0.0226	0.13
H200007028	S-100 binding protein, beta	0.0015	0.11
H200015420		0.0027	0.11
H200014979	Neutrophil gelatinase-associated lipocalin	0.0317	0.11

Figure 5-1 Characterization of NF-κB p50 stable clones. *A*, Western blot analysis of NF-κB p50 expression. NF-κB p50 is overexpressed in the stable clone M6 and M8 compared with the vector clone. *B*, Growth rate of vector clone and clones overexpressing NF-κB p50 (M6 and M8) by SRB assay.

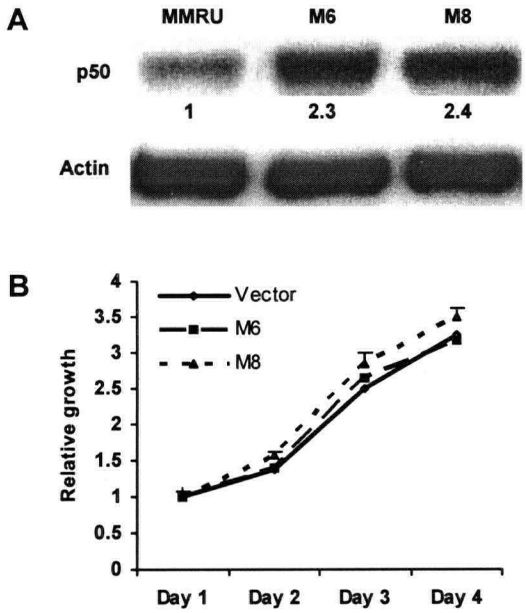

Figure 5-2 Cluster analysis of 179 genes showing alteration between p50-overexpressing M8 clone and vector clone through statistical analysis (*t*-test) and fold change criteria (≥2 folds). Levels of expression were presented on a scale from the lowest expression (dark green) to the highest expression (bright red).

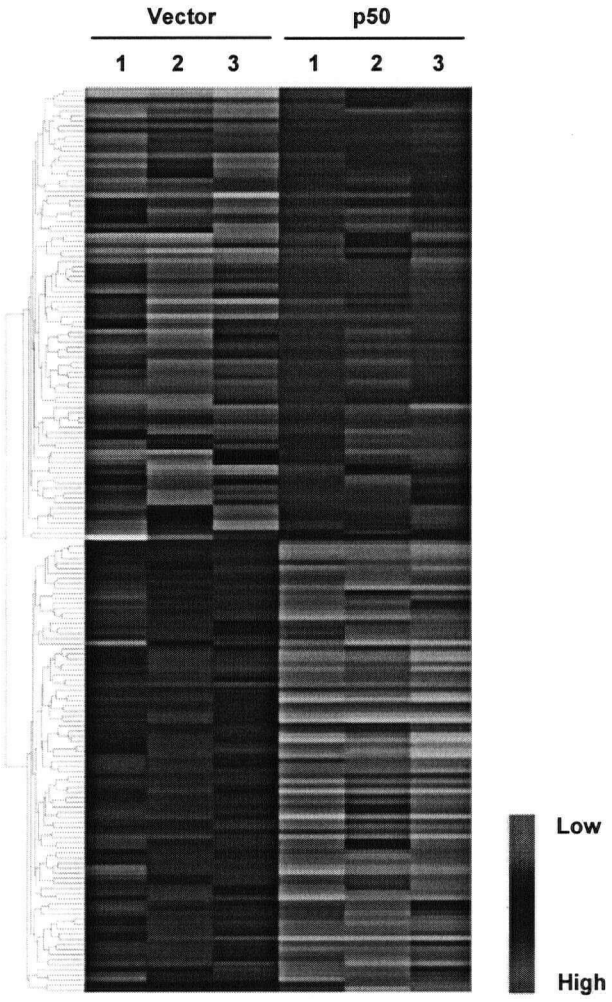

Figure 5-3. Validation of selected genes activated and inhibited by NF-κB p50 using quantitative real-time RT-PCR. Data are the amount of mRNA in p50 stable clone M8 relative to vector clone. Columns, mean of triplicate experiments; bars, SD.

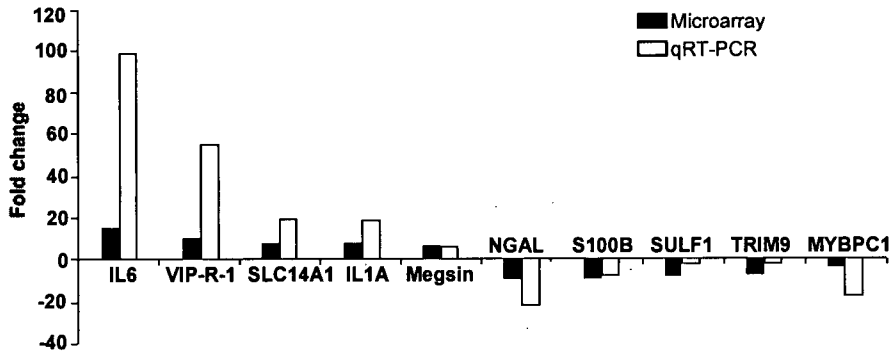

Figure 5-4. NF-κB p50 enhances angiogenesis *in vitro* and *in vivo*. *A*, Production of IL-6 in vector clone as well as p50-overexpressing clone M6 and M8, determined by ELISA. *B*, Relative rates of HUVECs proliferation stimulated by conditioned medium from vector clone (Vector-CM), p50-overexpressing clone M8 (p50-CM) and conditioned medium neutralized with IL-6 antibody (Vector-CM/IL-6 Ab and p50-CM/IL-6 Ab). *C*, NF-κB p50 promotes angiogenesis by the matrigel plug assay. *D*, Hemoglobin levels in the plugs were determined using Drabkin's solution. The experiments were performed in triplicate. Columns, means from triplicate experiments; bar, SD.

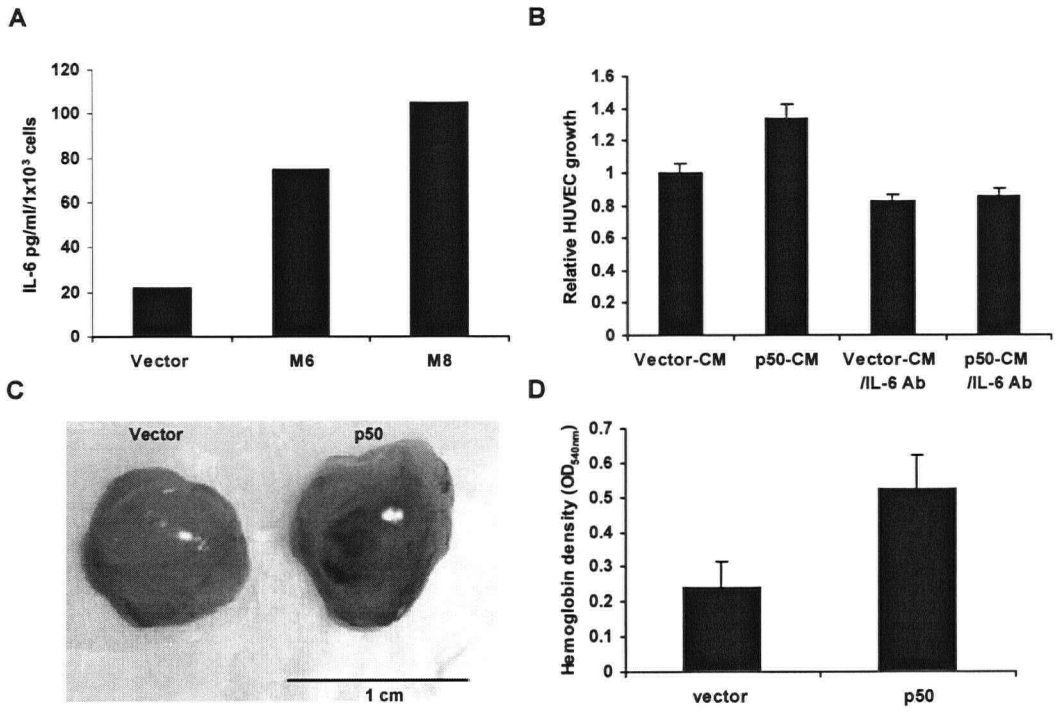

Figure 5-5 Knockdown of NF-κB p50 reduces IL-6 expression in MMRU melanoma cells. *A*, p105 shRNA knocked down p105 and p50, but not p65 in MMRU cells. *B* and *C*, IL-6 mRNA and protein levels were reduced by p105 shRNA measured by RT-PCR and ELISA, respectively. *D* and *E*, Overexpression of ATF3 abrogated the effect of p50 on the induction of IL-6 measured by conventional RT-PCR and ELISA, respectively.

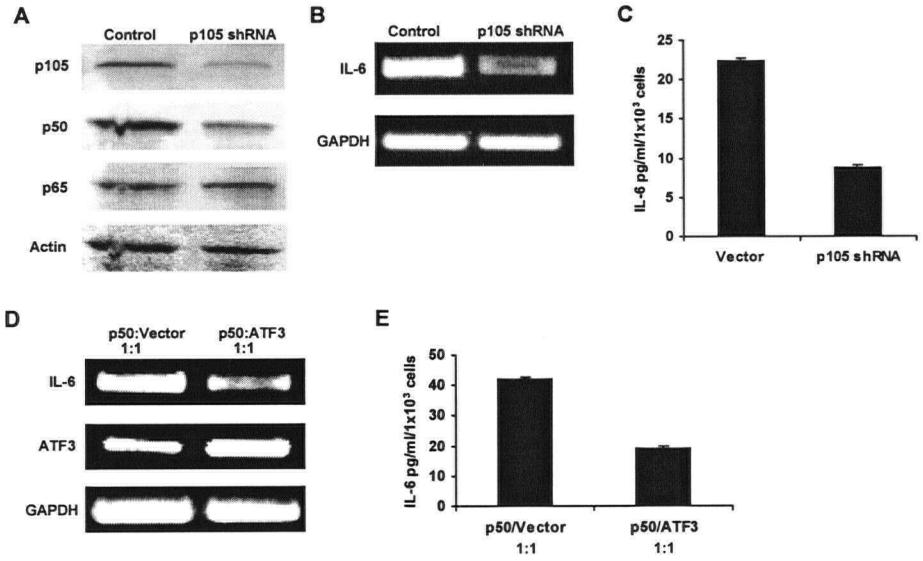

Chapter 6 Concluding remarks

Cutaneous melanoma is a highly aggressive skin cancer arising from malignant transformation of epidermal melanocytes as a result of complex interactions between constitutional, genetic, and environmental factors. Its incidence was increased by 3-8% annually in the Caucasian population. Although early-stage melanoma is curable with surgical excision, treatment for the advanced disease is ineffective and clinicians are in great need of new therapy.

Since aberrant activity of NF-κB has been a hallmark of many types of cancer including melanoma, targeting NF-κB in melanoma would be promising because studies have shown that NF-κB activity is important in melanoma proliferation, adhesion, antiapoptosis and metastasis. However, NF-κB also functions as anticancer factor in some occasions and controlling normal immunity and hematopoiesis. Therefore the functions of NF-κB would be dependent on the context of cell type and activity of NF-κB family members induced by various stresses.

In this study, we explored the role of NF-κB subunit p50 in melanoma pathogenesis. We first found the expression of NF-κB p50 was elevated in dysplastic nevi, primary melanoma, metastasic melanoma compared with normal nevi and the prognostic significance of strong nuclear staining of p50 in thick melanoma, which suggest that NF-κB p50 may be involved in vertical growth phase and cell motility. Next, we showed that NF-κB p50 promoted not only melanoma cell migration via enhancing RhoA activity, but also angiogenesis through upregulating IL-6 expression. These findings highlight

that NF-κB p50 play an important role in melanoma invasion and angiogenesis.

Future study would focus on investigation of the interaction of p50 with other transcription factors which are involved in regulation of downstream of p50 such as VIP-R-1 and IL-1 alpha. This work would contribute to the understanding of the regulatory mechanism of NF-κB in the cell. Mass spectrometer would be a powerful tool to identify the co-factors in the complex of p50. In addition, previous work shows that some factors such as ILK and PI3 kinase also promote cell migration. Therefore, it would be of interest to look for the relationship between p50 and these known factors, which may provide novel evidence on the mechanisms of cell migration.

On the other hand, the future *in vivo* study would emphasize on the therapeutic significance of NF-κB in melanoma. Since both NF-κB subunit p65 and p50 play an important role in melanoma pathogenesis, inhibition of their activity by specific RNAi would be a promising means to treat melanoma. To maximally eliminate the side effect of other types of cell, the adenovirus or lentivirus coding shRNA of p65 and p50 could be integrated with tyrosinase promoter, which is conditionally amplified and exerts the effect of downregulation of NF-κB in melanoma cells.

In summary, this work significantly contributed to the knowledge and understanding of NF-κB p50 in melanoma. The present results are exciting and promising, which would be valuable to explore the complex functions of NF-κB family members and provide the basis for novel therapies in melanoma.

References

Aggarwal, B. B. (2004). "Nuclear factor-kappaB: the enemy within." Cancer Cell 6(3): 203-8.

Alonso, S. R., P. Ortiz, et al. (2004). "Progression in cutaneous malignant melanoma is associated with distinct expression profiles: a tissue microarray-based study." Am J Pathol 164(1): 193-203.

Amiri, K. I., L. W. Horton, et al. (2004). "Augmenting chemosensitivity of malignant melanoma tumors via proteasome inhibition: implication for bortezomib (VELCADE, PS-341) as a therapeutic agent for malignant melanoma." Cancer Res 64(14): 4912-8.

Amiri, K. I. and A. Richmond (2005). "Role of nuclear factor-kappa B in melanoma." Cancer Metastasis Rev 24(2): 301-13.

Ara, T. and Y. A. DeClerck (2006). "Mechanisms of invasion and metastasis in human neuroblastoma." Cancer Metastasis Rev 25(4): 645-57.

Bakker, T. R., D. Reed, et al. (1999). "Efficient adenoviral transfer of NF-kappaB inhibitor sensitizes melanoma to tumor necrosis factor-mediated apoptosis." Int J Cancer 80(2): 320-3.

Baldwin, A. S., Jr. (1996). "The NF-kappa B and I kappa B proteins: new discoveries and insights." Annu Rev Immunol 14: 649-83.

Ballo, M. T. and K. K. Ang (2003). "Radiation therapy for malignant melanoma." Surg Clin North Am 83(2): 323-42.

Becker, J. C., J. M. Kirkwood, et al. (2006). "Molecularly targeted therapy for melanoma: current reality and future options." Cancer 107(10): 2317-27.

Beg, A. A., W. C. Sha, et al. (1995). "Embryonic lethality and liver degeneration in mice lacking the RelA component of NF-kappa B." Nature 376(6536): 167-70.

Bond, M., R. P. Fabunmi, et al. (1998). "Synergistic upregulation of metalloproteinase-9 by growth factors and inflammatory cytokines: an absolute requirement for transcription factor NF-kappa B." FEBS Lett 435(1): 29-34.

Borghaei, R. C., P. L. Rawlings, Jr., et al. (2004). "NF-kappaB binds to a polymorphic repressor element in the MMP-3 promoter." Biochem Biophys Res Commun 316(1): 182-8.

Boyano, M. D., M. D. Garcia-Vazquez, et al. (2000). "Soluble interleukin-2 receptor, intercellular adhesion molecule-1 and interleukin-10 serum levels in patients with melanoma." Br J Cancer 83(7): 847-52.

Burridge, K. and K. Wennerberg (2004). "Rho and Rac take center stage." Cell 116(2): 167-79.

Cao, S., X. Zhang, et al. (2006). "NF-kappaB1 (p50) homodimers differentially regulate pro- and anti-inflammatory cytokines in macrophages." J Biol Chem 281(36): 26041-50.

Cavarretta, I. T., H. Neuwirt, et al. (2006). "The antiapoptotic effect of IL-6 autocrine loop in a cellular model of advanced prostate cancer is mediated by Mcl-1." Oncogene.

Chen, X., K. Kandasamy, et al. (2003). "Differential roles of RelA (p65) and c-Rel subunits of nuclear factor kappa B in tumor necrosis factor-related apoptosis-inducing ligand signaling." Cancer Res 63(5): 1059-66.

Clark, E. A., T. R. Golub, et al. (2000). "Genomic analysis of metastasis reveals an essential role for RhoC." Nature 406(6795): 532-5.

Cornil, I., D. Theodorescu, et al. (1991). "Fibroblast cell interactions with human melanoma cells affect tumor cell growth as a function of tumor progression." Proc Natl Acad Sci U S A 88(14): 6028-32.

Culig, Z., H. Steiner, et al. (2005). "Interleukin-6 regulation of prostate cancer cell growth." J Cell Biochem 95(3): 497-505.

Dai, D. L., M. Martinka, et al. (2005). "Prognostic significance of activated Akt expression in melanoma: a clinicopathologic study of 292 cases." J Clin Oncol 23(7): 1473-82.

Dajee, M., M. Lazarov, et al. (2003). "NF-kappaB blockade and oncogenic Ras trigger invasive human epidermal neoplasia." Nature 421(6923): 639-43.

Denkert, C., M. Kobel, et al. (2001). "Expression of cyclooxygenase 2 in human malignant melanoma." Cancer Res 61(1): 303-8.

Deveraux, Q. L., N. Roy, et al. (1998). "IAPs block apoptotic events induced by caspase-8 and cytochrome c by direct inhibition of distinct caspases." Embo J 17(8): 2215-23.

Domingo-Domenech, J., C. Oliva, et al. (2006). "Interleukin 6, a nuclear factor-kappaB target, predicts resistance to docetaxel in hormone-independent prostate cancer and nuclear factor-kappaB inhibition by PS-1145 enhances docetaxel antitumor activity." Clin Cancer Res 12(18): 5578-86.

Eigentler, T. K., U. M. Caroli, et al. (2003). "Palliative therapy of disseminated malignant melanoma: a systematic review of 41 randomised clinical trials." Lancet Oncol 4(12): 748-59.

Erhard, H., F. J. Rietveld, et al. (1997). "Transition of horizontal to vertical growth phase melanoma is accompanied by induction of vascular endothelial growth factor expression and angiogenesis." Melanoma Res 7 Suppl 2: S19-26.

Feinman, R., J. Koury, et al. (1999). "Role of NF-kappaB in the rescue of multiple myeloma cells from glucocorticoid-induced apoptosis by bcl-2." Blood 93(9): 3044-52.

Finco, T. S., J. K. Westwick, et al. (1997). "Oncogenic Ha-Ras-induced signaling activates NF-kappaB transcriptional activity, which is required for cellular transformation." J Biol Chem 272(39): 24113-6.

Florenes, V. A., C. Lu, et al. (1999). "Interleukin-6 dependent induction of the cyclin dependent kinase inhibitor p21WAF1/CIP1 is lost during progression of human malignant melanoma." Oncogene 18(4): 1023-32.

Fox, C. J., P. S. Hammerman, et al. (2003). "The serine/threonine kinase Pim-2 is a transcriptionally regulated apoptotic inhibitor." Genes Dev 17(15): 1841-54.

Franco, A. V., X. D. Zhang, et al. (2001). "The role of NF-kappa B in TNF-related apoptosis-inducing ligand (TRAIL)-induced apoptosis of melanoma cells." J Immunol 166(9): 5337-45.

Gao, K., D. L. Dai, et al. (2006). "Prognostic Significance of Nuclear Factor-{kappa}B p105/p50 in Human Melanoma and Its Role in Cell Migration." Cancer Res 66(17): 8382-8.

Garkavtsev, I., S. V. Kozin, et al. (2004). "The candidate tumour suppressor protein ING4 regulates brain tumour growth and angiogenesis." Nature 428(6980): 328-32.

Gassmann, P., A. Enns, et al. (2004). "Role of tumor cell adhesion and migration in organ-specific metastasis formation." Onkologie 27(6): 577-82.

Ghiorzo, P., M. Mantelli, et al. (2004). "Inverse correlation between p16INK4A expression and NF-kappaB activation in melanoma progression." Hum Pathol 35(8): 1029-37.

Ghosh, S., M. J. May, et al. (1998). "NF-kappa B and Rel proteins: evolutionarily conserved mediators of immune responses." Annu Rev Immunol 16: 225-60.

Gilchrist, M., V. Thorsson, et al. (2006). "Systems biology approaches identify ATF3 as a negative regulator of Toll-like receptor 4." Nature 441(7090): 173-8.

Gray-Schopfer, V., C. Wellbrock, et al. (2007). "Melanoma biology and new targeted therapy." Nature 445(7130): 851-7.

Grossman, D. and D. C. Altieri (2001). "Drug resistance in melanoma: mechanisms, apoptosis, and new potential therapeutic targets." Cancer Metastasis Rev 20(1-2): 3-11.

Guan, H., S. Hou, et al. (2005). "DNA binding of repressor nuclear factor-kappaB p50/p50 depends on phosphorylation of Ser337 by the protein kinase A catalytic subunit." J Biol Chem 280(11): 9957-62.

Hall, A. (1998). "Rho GTPases and the actin cytoskeleton." Science 279(5350): 509-14.

Hanahan, D. and R. A. Weinberg (2000). "The hallmarks of cancer." Cell 100(1): 57-70.

Haussler, U., G. von Wichert, et al. (2005). "Epidermal growth factor activates nuclear factor-kappaB in human proximal tubule cells." Am J Physiol Renal Physiol 289(4): F808-15.

Heinrich, P. C., I. Behrmann, et al. (2003). "Principles of interleukin (IL)-6-type cytokine signalling and its regulation." Biochem J 374(Pt 1): 1-20.

Hendrix, M. J., E. A. Seftor, et al. (2003). "Molecular plasticity of human melanoma cells." Oncogene 22(20): 3070-5.

Hersey, P. (2003). "Adjuvant therapy for high-risk primary and resected metastatic melanoma." Intern Med J 33(1-2): 33-43.

Horwitz, R. and D. Webb (2003). "Cell migration." Curr Biol 13(19): R756-9.

Huang, S. P., M. S. Wu, et al. (2004). "Interleukin-6 increases vascular endothelial growth factor and angiogenesis in gastric carcinoma." J Biomed Sci 11(4): 517-27.

Iademarco, M. F., J. J. McQuillan, et al. (1992). "Characterization of the promoter for vascular cell adhesion molecule-1 (VCAM-1)." J Biol Chem 267(23): 16323-9.

Ivanov, V. N. and T. K. Hei (2005). "Combined treatment with EGFR inhibitors and arsenite upregulated apoptosis in human EGFR-positive melanomas: a role of suppression of the PI3K-AKT pathway." Oncogene 24(4): 616-26.

Jaffe, A. B. and A. Hall (2005). "Rho GTPases: biochemistry and biology." Annu Rev Cell Dev Biol 21: 247-69.

Jee, S. H., C. Y. Chu, et al. (2004). "Interleukin-6 induced basic fibroblast growth factor-dependent angiogenesis in basal cell carcinoma cell line via JAK/STAT3 and PI3-kinase/Akt pathways." J Invest Dermatol 123(6): 1169-75.

Jemal, A., R. Siegel, et al. (2006). "Cancer statistics, 2006." CA Cancer J Clin 56(2): 106-30.

Jemal, A., A. Thomas, et al. (2002). "Cancer statistics, 2002." CA Cancer J Clin 52(1): 23-47.

Jenkins, G. J., J. Mikhail, et al. (2007). "Immunohistochemical study of NF-kB activity and IL-8 abundance in oesophageal adenocarcinoma; a useful strategy for monitoring these biomarkers." J Clin Pathol.

Jimenez, C., R. A. Portela, et al. (2000). "Role of the PI3K regulatory subunit in the control of actin organization and cell migration." J Cell Biol 151(2): 249-62.

Johnson, J. P., B. G. Stade, et al. (1989). "De novo expression of intercellular-adhesion molecule 1 in melanoma correlates with increased risk of metastasis." Proc Natl Acad Sci U S A 86(2): 641-4.

Jones, S. A., S. Horiuchi, et al. (2001). "The soluble interleukin 6 receptor: mechanisms of production and implications in disease." Faseb J 15(1): 43-58.

Kallen, K. J. (2002). "The role of transsignalling via the agonistic soluble IL-6 receptor in human diseases." Biochim Biophys Acta 1592(3): 323-43.

Karin, M. and Y. Ben-Neriah (2000). "Phosphorylation meets ubiquitination: the control of NF-[kappa]B activity." Annu Rev Immunol 18: 621-63.

Karin, M. and A. Lin (2002). "NF-kappaB at the crossroads of life and death." Nat Immunol 3(3): 221-7.

Kashani-Sabet, M., R. W. Sagebiel, et al. (2002). "Tumor vascularity in the prognostic assessment of primary cutaneous melanoma." J Clin Oncol 20(7): 1826-31.

Kashani-Sabet, M., L. Shaikh, et al. (2004). "NF-kappa B in the vascular progression of melanoma." J Clin Oncol 22(4): 617-23.

Kawano, M., T. Hirano, et al. (1988). "Autocrine generation and requirement of BSF-2/IL-6 for human multiple myelomas." Nature 332(6159): 83-5.

Kim, D. W., L. Gazourian, et al. (2000). "The RelA NF-kappaB subunit and the aryl hydrocarbon receptor (AhR) cooperate to transactivate the c-myc promoter in mammary cells." Oncogene 19(48): 5498-506.

Kojima, S., D. J. Mulholland, et al. (2006). "Differential regulation of IGFBP-3 by the androgen receptor in the lineage-related androgen-dependent LNCaP and androgen-independent C4-2 prostate cancer models." Prostate 66(9): 971-86.

Kunz, M., A. Hartmann, et al. (1999). "Anoxia-induced up-regulation of interleukin-8 in human malignant melanoma. A potential mechanism for high tumor aggressiveness." Am J Pathol 155(3): 753-63.

Kuo, M. T., Z. Liu, et al. (2002). "Induction of human MDR1 gene expression by 2-acetylaminofluorene is mediated by effectors of the phosphoinositide 3-kinase pathway that activate NF-kappaB signaling." Oncogene 21(13): 1945-54.

Labrousse, A. L., C. Ntayi, et al. (2004). "Stromal reaction in cutaneous melanoma." Crit Rev Oncol Hematol 49(3): 269-75.

Langley, R. R., R. Carlisle, et al. (2001). "Endothelial expression of vascular cell adhesion molecule-1 correlates with metastatic pattern in spontaneous melanoma." Microcirculation 8(5): 335-45.

Leung, T. H., A. Hoffmann, et al. (2004). "One nucleotide in a kappaB site can determine cofactor specificity for NF-kappaB dimers." Cell 118(4): 453-64.

Levine, L., J. A. Lucci, 3rd, et al. (2003). "Bombesin stimulates nuclear factor kappa B activation and expression of proangiogenic factors in prostate cancer cells." Cancer Res 63(13): 3495-502.

Ling, M. T., X. Wang, et al. (2004). "Id-1 expression induces androgen-independent prostate cancer cell growth through activation of epidermal growth factor receptor (EGF-R)." Carcinogenesis 25(4): 517-25.

Lu, C. and R. S. Kerbel (1993). "Interleukin-6 undergoes transition from paracrine growth inhibitor to autocrine stimulator during human melanoma progression." J Cell Biol 120(5): 1281-8.

Ma, L., P. del Soldato, et al. (2002). "Divergent effects of new cyclooxygenase inhibitors on gastric ulcer healing: Shifting the angiogenic balance." Proc Natl Acad Sci U S A 99(20): 13243-7.

Maekawa, M., T. Ishizaki, et al. (1999). "Signaling from Rho to the actin cytoskeleton through protein kinases ROCK and LIM-kinase." Science 285(5429): 895-8.

Maffucci, T., F. T. Cooke, et al. (2005). "Class II phosphoinositide 3-kinase defines a novel signaling pathway in cell migration." J Cell Biol 169(5): 789-99.

Marghoob, A. A., K. Koenig, et al. (2000). "Breslow thickness and clark level in melanoma: support for including level in pathology reports and in American Joint Committee on Cancer Staging." Cancer 88(3): 589-95.

Mathas, S., K. Johrens, et al. (2005). "Elevated NF-kappaB p50 complex formation and Bcl-3 expression in classical Hodgkin, anaplastic large-cell, and other peripheral T-cell lymphomas." Blood 106(13): 4287-93.

McNulty, S. E., R. del Rosario, et al. (2004). "Comparative expression of NFkappaB proteins in melanocytes of normal skin vs. benign intradermal naevus and human metastatic melanoma biopsies." Pigment Cell Res 17(2): 173-80.

McNulty, S. E., N. B. Tohidian, et al. (2001). "RelA, p50 and inhibitor of kappa B alpha are elevated in human metastatic melanoma cells and respond aberrantly to ultraviolet light B." Pigment Cell Res 14(6): 456-65.

Meng, F., Y. Yamagiwa, et al. (2005). "IL-6 activates serum and glucocorticoid kinase via p38alpha mitogen-activated protein kinase pathway." Am J Physiol Cell Physiol 289(4): C971-81.

Montaner, S., R. Perona, et al. (1998). "Multiple signalling pathways lead to the activation of the nuclear factor kappaB by the Rho family of GTPases." J Biol Chem 273(21): 12779-85.

Narita, K., J. Staub, et al. (2006). "HSulf-1 inhibits angiogenesis and tumorigenesis in vivo." Cancer Res 66(12): 6025-32.

Natoli, G., S. Saccani, et al. (2005). "Interactions of NF-kappaB with chromatin: the art of being at the right place at the right time." Nat Immunol 6(5): 439-45.

Ng, K. C., E. I. Campos, et al. (2004). "XAF1 expression is significantly reduced in human melanoma." J Invest Dermatol 123(6): 1127-34.

Nicolini, A., A. Carpi, et al. (2006). "Cytokines in breast cancer." Cytokine Growth Factor Rev 17(5): 325-37.

Nilsson, M. B., R. R. Langley, et al. (2005). "Interleukin-6, secreted by human ovarian carcinoma cells, is a potent proangiogenic cytokine." Cancer Res 65(23): 10794-800.

Novak, U., B. G. Cocks, et al. (1991). "A labile repressor acts through the NFkB-like binding sites of the human urokinase gene." Nucleic Acids Res 19(12): 3389-93.

Perona, R., S. Montaner, et al. (1997). "Activation of the nuclear factor-kappaB by Rho, CDC42, and Rac-1 proteins." Genes Dev 11(4): 463-75.

Prusty, B. K., S. A. Husain, et al. (2005). "Constitutive activation of nuclear factor -kB: preferntial homodimerization of p50 subunits in cervical carcinoma." Front Biosci 10: 1510-9.

Ravi, R., G. C. Bedi, et al. (2001). "Regulation of death receptor expression and TRAIL/Apo2L-induced apoptosis by NF-kappaB." Nat Cell Biol 3(4): 409-16.

Ren, X. D., W. B. Kiosses, et al. (1999). "Regulation of the small GTP-binding protein Rho by cell adhesion and the cytoskeleton." Embo J 18(3): 578-85.

Ridley, A. J., M. A. Schwartz, et al. (2003). "Cell migration: integrating signals from front to back." Science 302(5651): 1704-9.

Schmidt, A. and A. Hall (2002). "Guanine nucleotide exchange factors for Rho GTPases: turning on the switch." Genes Dev 16(13): 1587-609.

Schumm, K., S. Rocha, et al. (2006). "Regulation of p53 tumour suppressor target gene expression by the p52 NF-kappaB subunit." Embo J 25(20): 4820-32.

Serrone, L., M. Zeuli, et al. (2000). "Dacarbazine-based chemotherapy for metastatic melanoma: thirty-year experience overview." J Exp Clin Cancer Res 19(1): 21-34.

Shattuck-Brandt, R. L. and A. Richmond (1997). "Enhanced degradation of I-kappaB alpha contributes to endogenous activation of NF-kappaB in Hs294T melanoma cells." Cancer Res 57(14): 3032-9.

Soengas, M. S. and S. W. Lowe (2003). "Apoptosis and melanoma chemoresistance." Oncogene 22(20): 3138-51.

Sosman, J. A. and I. Puzanov (2006). "Molecular targets in melanoma from angiogenesis to apoptosis." Clin Cancer Res 12(7 Pt 2): 2376s-2383s.

Sovak, M. A., R. E. Bellas, et al. (1997). "Aberrant nuclear factor-kappaB/Rel expression and the pathogenesis of breast cancer." J Clin Invest 100(12): 2952-60.

Sparmann, A. and D. Bar-Sagi (2004). "Ras-induced interleukin-8 expression plays a critical role in tumor growth and angiogenesis." Cancer Cell 6(5): 447-58.

Streit, M. and M. Detmar (2003). "Angiogenesis, lymphangiogenesis, and melanoma metastasis." Oncogene 22(20): 3172-9.

Su, J. L., K. P. Lai, et al. (2005). "A novel peptide specifically binding to interleukin-6 receptor (gp80) inhibits angiogenesis and tumor growth." Cancer Res 65(11): 4827-35.

Suh, J. and A. B. Rabson (2004). "NF-kappaB activation in human prostate cancer: important mediator or epiphenomenon?" J Cell Biochem 91(1): 100-17.

Suyama, E., H. Kawasaki, et al. (2004). "Cell migration and metastasis as targets of small RNA-based molecular genetic analyses." J Muscle Res Cell Motil 25(4-5): 303-8.

Taga, T. and T. Kishimoto (1997). "Gp130 and the interleukin-6 family of cytokines." Annu Rev Immunol 15: 797-819.

Thomsen, L. L. and D. W. Miles (1998). "Role of nitric oxide in tumour progression: lessons from human tumours." Cancer Metastasis Rev 17(1): 107-18.

Thornburg, N. J., R. Pathmanathan, et al. (2003). "Activation of nuclear factor-kappaB p50 homodimer/Bcl-3 complexes in nasopharyngeal carcinoma." Cancer Res 63(23): 8293-301.

Ueda, Y. and A. Richmond (2006). "NF-kappaB activation in melanoma." Pigment Cell Res 19(2): 112-24.

van de Stolpe, A., E. Caldenhoven, et al. (1994). "12-O-tetradecanoylphorbol-13-acetate- and tumor necrosis factor alpha-mediated induction of intercellular adhesion molecule-1 is inhibited by dexamethasone. Functional analysis of the human intercellular adhesion molecular-1 promoter." J Biol Chem 269(8): 6185-92.

van den Oord, J. J., L. Paemen, et al. (1997). "Expression of gelatinase B and the extracellular matrix metalloproteinase inducer EMMPRIN in benign and malignant pigment cell lesions of the skin." Am J Pathol 151(3): 665-70.

Wang, W., J. L. Abbruzzese, et al. (1999). "Overexpression of urokinase-type plasminogen activator in pancreatic adenocarcinoma is regulated by constitutively activated RelA." Oncogene 18(32): 4554-63.

Wang, X., K. Belguise, et al. (2007). "Oestrogen signalling inhibits invasive phenotype by repressing RelB and its target BCL2." Nat Cell Biol 9(4): 470-8.

Wang, Y. and G. Li (2006). "ING3 promotes UV-induced apoptosis via Fas/caspase-8 pathway in melanoma cells." J Biol Chem 281(17): 11887-93.

Warren, B. A. and P. Shubik (1966). "The growth of the blood supply to melanoma transplants in the hamster cheek pouch." Lab Invest 15(2): 464-78.

Wheeler, A. P. and A. J. Ridley (2004). "Why three Rho proteins? RhoA, RhoB, RhoC, and cell motility." Exp Cell Res 301(1): 43-9.

Whelan, J., P. Ghersa, et al. (1991). "An NF kappa B-like factor is essential but not sufficient for cytokine induction of endothelial leukocyte adhesion molecule 1 (ELAM-1) gene transcription." Nucleic Acids Res 19(10): 2645-53.

Yang, J. and A. Richmond (2001). "Constitutive IkappaB kinase activity correlates with nuclear factor-kappaB activation in human melanoma cells." Cancer Res 61(12): 4901-9.

Yao, J. S., W. Zhai, et al. (2006). "Interleukin-6 triggers human cerebral endothelial cells proliferation and migration: the role for KDR and MMP-9." Biochem Biophys Res Commun 342(4): 1396-404.

Ziegler-Heitbrock, L. (2001). "The p50-homodimer mechanism in tolerance to LPS." J Endotoxin Res 7(3): 219-22.